Table of Contents - Issue 25, Summer 2007

Full Papers:

Tests for Evaluating the Ignitability of Firework Stars and Compositions 3

Yasuhiro Sashimura, Mamoru Horiuchi, Hideo Watanabe, Maiko Watanabe, Dayu Ding and Tadao Yoshida

Spectroscopic Measurement of Burning Toy Fireworks 14

Kazuomi Itoh, Dayu Ding and Tadao Yoshida

Burning Characteristics of Firework Stars and Lifting Charge 28

Morimasa Higaki, Dayu Ding, Yuzo Ooki and Tadao Yoshida

Exterior Ballistics of Firework Stars 37

Yuzo Ooki, Dayu Ding, Morimasa Higaki and Tadao Yoshida

Evaluation Of Multi-shot Firework Articles Using Mortar Recoil Measurements 44

R. Guilbeault and E. Contestabile

Communications, Short Papers and Book Reviews:

Survey of Firework Trends from UK Display Companies 49

Tom Smith and Avril diPalma

Thermal Conductivity Testing of Minimal Volumes of Energetic Powders 53

Adam Harris and Daniel N. Sorensen

Review of: Introduction to Fireworks – T Yoshida and D Ding 58

Reviewed by Theodore S. Sumrall

Review of: Bombs and Bombings, A Handbook to Protection, Security, Detection, Disposal, and Investigation for Industry, Police, and Fire Departments, Third Edition. – Thomas G. Brodie 59

Reviewed by Megan Bottegal and Bruce McCord

Events Calendar 59

Sponsors 60

Information for Authors 64

Journal of Pyrotechnics

Production Team

Publisher
Tom Smith
Davas Ltd
8 Aragon Place, Kimbolton
Huntingdon, Cambs
PE28 0JD, UK

Phone: +44 1480 860124
Fax: +44 1480 861108
email: toms@davas.co.uk

Production Editor
Helen Saxton
Davas Ltd
8 Aragon Place, Kimbolton
Huntingdon, Cambs
PE28 0JD, UK

Phone: +44 1480 860124
Fax: +44 1480 861108
email: helens@davas.co.uk

Publishing Consultant
Bonnie Kosanke
1775 Blair Road,
Whitewater
CO 81527, USA

Phone: +1-970-245-0692
Fax: +1-970-245-0692
email: bonnie@jpyro.com

Tests for Evaluating the Ignitability of Firework Stars and Compositions

Yasuhiro Sashimura[a], Mamoru Horiuchi,[b] Hideo Watanabe,[b] Maiko Watanabe,[b] Dayu Ding[b] and Tadao Yoshida[b]*

[a] 1-27-14-201 Matumi-cho, Kanagawa-ku, Yokohama-shi, Japan

[b] Ashikaga Institute of Technology

268-1 Omae-cho, Ashikaga-shi, Tochigi 326-8558, Japan

Tel: +81-284-62-0605, fax: +81-284-62-0976, email: yoshida@ashitech.ac.jp

* To whom all correspondence should be addressed.

Abstract: *A shot test was examined for evaluating the ignitability of cylindrical bare and primed stars. The primed stars were more easily ignited than the bare stars. The ignition limit lift charge was defined and used for evaluating the ignitability. Though the ignition limit lift charges of the primed stars were widely scattered, the order of average ignitability of primed stars was: F > J > D > C > L > G > A > E > H > K > I > B The order of ignitability of bare stars was: blue star > yellow star > purple star > green star > red star. The hot plate and electric match tests were carried out for screening the ignitability of star, prime, lifting charge and bursting charge compositions. Both the test methods may be applied to screen the ignitability of bare star compositions from the other more ignitable compositions though there are rare exceptions.*

Keywords: *fireworks, ignitability, shot test, hot plate test, electric match test, prime, star, lifting charge, bursting charge*

Introduction

Fireworks give various effects by means of the combustion of the stars and compositions. The ignitability of the stars and compositions is important from the point of view of safety and performance of the fireworks. Too high an ignitability may cause a fire and explosion accident. Too low an ignitability may cause a misfire and a firework cannot work properly when one of the components is too insensitive to an igniter.

Ignitability tests of energetic materials including pyrotechnics were developed mainly for safety.[1,2] BAM in Germany developed several test methods for evaluating the ignitability of energetic materials. These methods include the cerium–iron spark, fuse, small gas flame, hot iron rod and hot bowl tests.[3] In Japan, the hot hole test has been used as a heat sensitivity test for energetic materials.[4]

Misfires of the fuse of a shell, the lifting and bursting charges, and stars have been suggested as causes of firework incidents. The misfires may be caused by the too low ignitability of those components of fireworks. In order to improve the ignitability of bare stars, the prime has been used. Kosanke and Kosanke have explained primes and priming.[5] We started to study the ignitability of these components using three tests: shot test, hot plate test and electric match test. Sashimura *et al.*[6] carried out a shot test for evaluating the ignitability of bare and primed stars of compositions cited in the literature.[7]

The shot test was referred to but details are not known except for Sashimura's work. The hot plate test used in this work is a similar method to the BAM hot bowl and Japanese hot hole tests. The electric match test is similar to the cerium–iron spark test in principle. In this article, those methods are applied to the compositions of prime, star, lifting and bursting charges.

Experimental

Materials

The sample compositions of stars and primes tested were prepared by the present authors and are listed in Tables 1 and 2, respectively. The lift and burst charges were supplied by Sunaga Fireworks Co. Ltd. The cylindrical bare and primed stars were

Table 1 *Compositions of bare stars.*

	Red star	Yellow star	Green star	Blue star	Purple star
$KClO_4$	53	48		62	53
$SrCO_3$	12				7
$K_2Cr_2O_7$		1	1		
$BaCO_3$		10			
$Ba(NO_3)_2$			54		
CuO				12	9
MgAl 180 mesh	15				
MgAl fine		15	20	1	8
Rice granules	5	5	5	4	5
Chlorinated gum	6		8	8	5
PVC	4	8		2	5
Phenol resin	3			10	8
Red gum	2	10	9		
Hemp charcoal			1	1	
Cryolite		3			

manufactured by Alps Fireworks Co. Ltd. Cross-section models of bare and primed stars are shown Figure 1. The bare star is 11 mm in diameter and about 10 mm long. The primed star is covered by a prime layer on the bare star.

The powdery compositions were wetted with 10% water and pressed into a square rod 1.5 × 5 mm in cross section by 30 mm in length, and then cut into 1.5 × 5 × 5 mm pieces. The pieces were dried in the open air.

Table 2. *Compositions of primes.*

Prime	A*	B	C	D	E	F	G	H	I	J	K	L
KNO_3	75	75	80	75	75	75	75	80	80	80	80	56
Hemp charcoal	15	15	20	15	15	15	15	20	20	20	20	9
S	10	10		10	10	10	10					5
Rice granules	5	5	5	5	5	5	5	5	5	5	5	7
MgAl 180 mesh				11				11				
MgAl fine												9
Al VA150					11				11			
Ti fine						11				11		
Si 200 mesh							11				11	
$K_2Cr_2O_7$				1				1				5
H_3BO_3					1				1			
Sb_2S_3												9

*Commercial black powder.

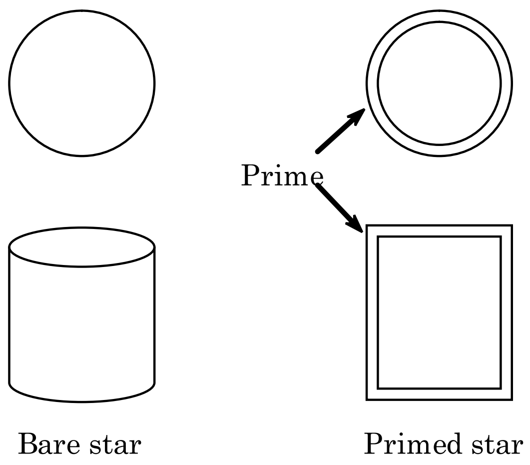

Figure 1. *Star samples.*

The electric match for the electric match test is a product of Nippon Kayaku Co. Ltd. The electric bridge wire of the electric match is made of a platinum–iridium alloy, about 0.03 mm in diameter and 300–400 Ω in electric resistance. The ignition charge is an equal mixture of lead thiocyanate and potassium perchlorate , and 12±3 mg in mass.

Apparatus

The setup of the shot test is shown in Figure 2. The mortar is a steel tube 270 mm long and 15 mm in inner diameter. The setup of the test apparatus for the ignitability test using a hot plate is shown in Figure 3. The apparatus consists of a 300 W electric Ni–Cr heater, 140 mm Ø × 1.0 mm steel plate, thermocouples, 140mm Ø × 40 mm heat insulating half-cut bricks. The heater was heated by an electric current through a transformer. The surface temperature of the hot plate was measured by a digital thermometer through the thermocouples attached on the plate. A high-speed video camera (Phantom VR-V4.2) was used for measuring the drop and ignition times of a sample piece.

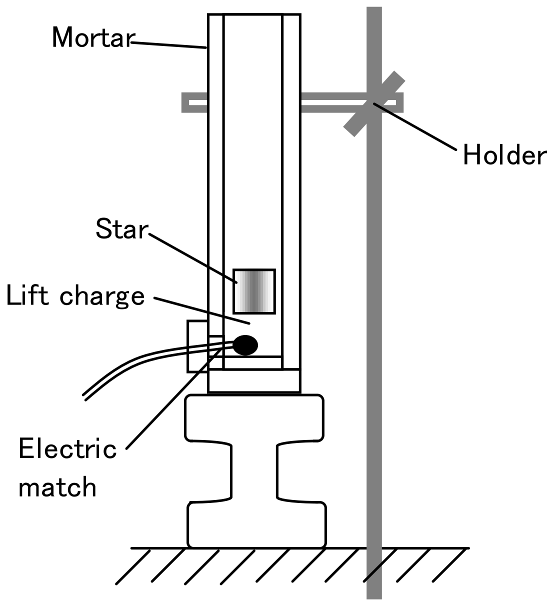

Figure 2. *Setup of shot test.*

The setup of the ignitability test using an electric match is shown in Figure 4.

Procedure for the shot test

An electric match is inserted into the bottom of mortar, which is fixed perpendicularly, the lift charge is poured into the mortar, and a star is dropped on the lift charge. The lift charge is ignited and the star is shot into the air, and the ignition or absence of ignition of the star is examined by observation by eye.

The star does not ignite when the lift charge is large, and the star does ignite when the lift charge is smaller. The mean of maximum lift charge for ignition and minimum lift charge for no ignition is defined as the ignition limit lift charge for an ignitability scale:

The ignition limit lift charge = (maximum lift charge for ignition + minimum lift charge for no ignition)/2

The test starts with a lift charge near the ignition limit lift charge, the lift charge is increased when there is ignition, and it is decreased when there is no ignition by 1 g increments above 1 g lift charge and 0.1 g increments below 1 g lift charge.

Procedure for the ignitability test using a hot plate

The steel plate was heated to 600 ºC, 650 ºC, 700 ºC, 750 ºC or 800 ºC, and the temperature maintained by adjusting the voltage of the transformer. A piece of sample was dropped on to the surface of the hot plate through a hole in the insulating brick. The experiment for each sample at the same temperature was repeated 5 times. The time of the drop and ignition of the sample was observed through an opening between the plate and the brick, and recorded by the high-speed

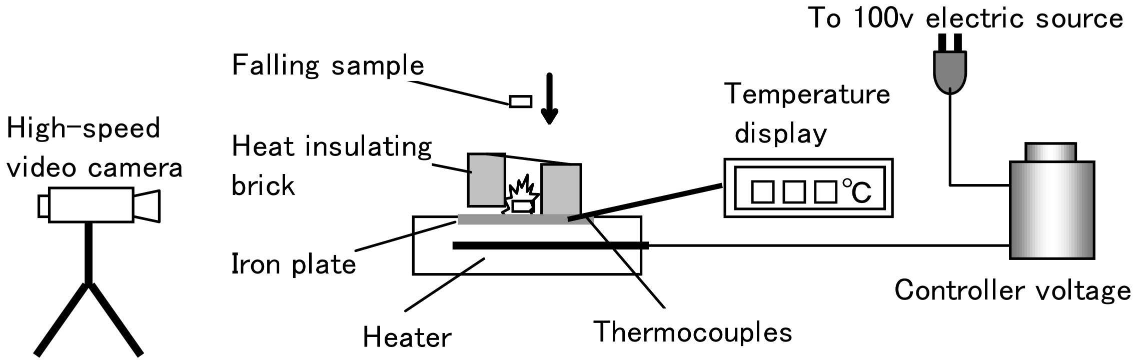

Figure 3. *Schematic diagram of ignitability test using a hot plate.*

video camera.

Procedure for the ignitability test using an electric match

A 1.5 × 5 × 5 mm sample and an electric match were wrapped together by a sheet of 3M Scotch green mending tape 10 mm wide and 30 mm long. The blue tape is not suitable because the confinement by the blue tape is weaker than that of the green tape. The wrapped sample was put on a heat resistant brick and covered with a transparent cup. A 12 V electric current was passed through the electric match and the match ignited. The tests were carried out 10 times and the number of ignitions was recorded.

Results and Discussion

Ignition limit lift charge of bare and primed stars

The results of the shot test of bare and primed stars are listed in Table 3. The order of the ignition limit lift charge of bare stars with (ignition limit lift charge) is as follows:

Yellow star (0.5 g) = purple star (0.5 g) > green star (0.3 g) = blue star (0.3 g) > red star (0.15 g)

The ignition limit lift charges of primed stars were scattered widely and therefore exact discussion is difficult. The mean values were in the following order:

Primed blue star (5.4 g) > primed yellow star (4.5 g) > primed purple star (4.3 g) > primed green star (4.0 g) > primed red star (3.1 g)

Figure 5 shows the plot of ignition limit lift charge of primed stars vs. that of bare stars. The ignition limit lift charges of primed stars were scattered widely but without exception were larger than those of bare stars. That is, the ignitability of primed stars was larger than that of bare stars, and the primers were all effective for promoting ignitability of bare stars. There is a relationship between the mean ignition limit lift charge of primed stars and the ignition limit lift charge of bare stars, and the ignitability of bare stars is

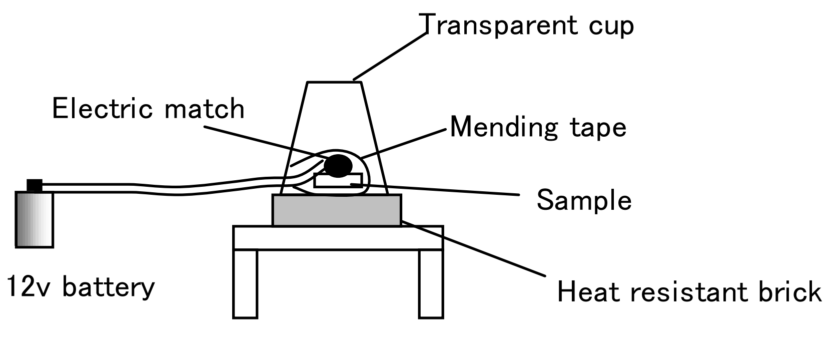

Figure 4. *Schematic diagram of ignitability test using an electric match.*

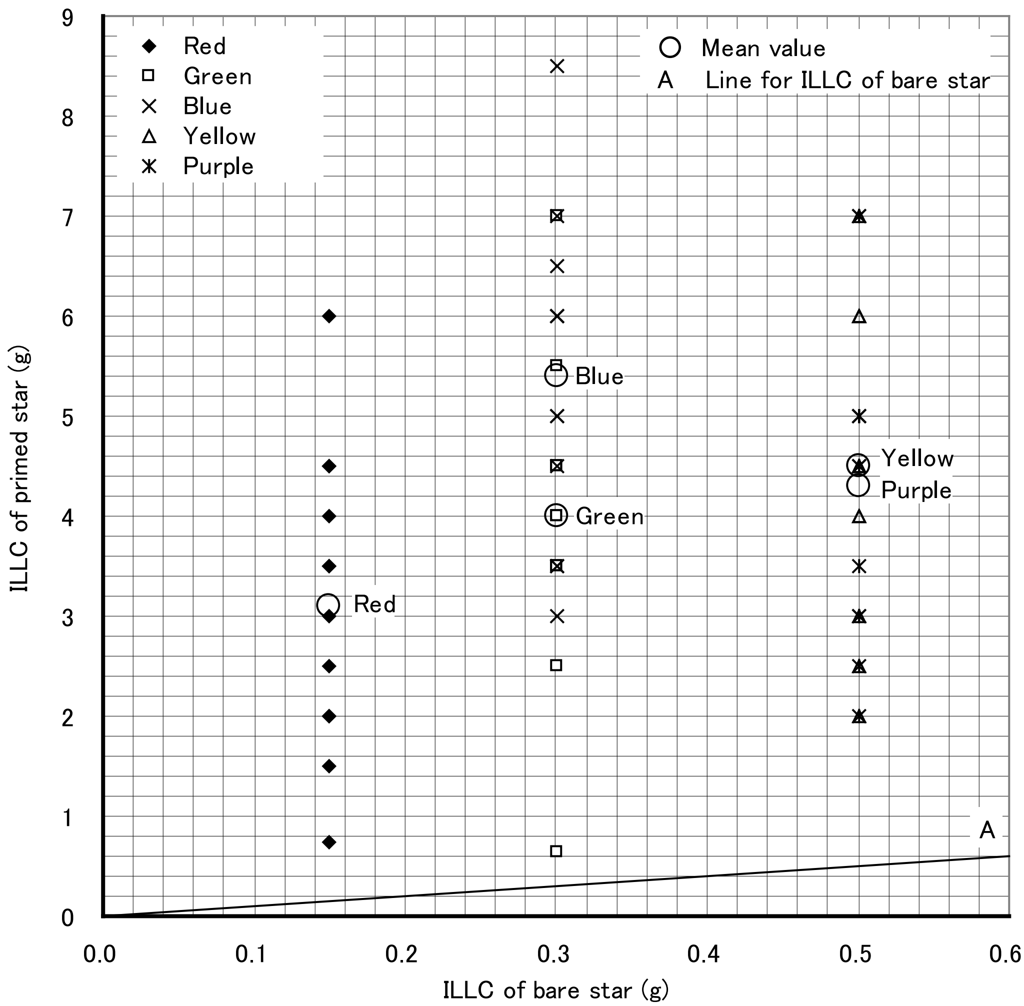

Figure 5. *Plot of ignition limit of lift charge (ILLC) of primed star vs. that of bare star.*

recognized to affect that of the primed star to a certain extent.

The order of ignitability of primers is difficult to judge because of the large scatter of the data. The order of mean ignition limit lift charge of primes was as follows:

F (5.5 g) > J (4.9 g) > D (4.8 g) > C (4.7 g) > L (4.6 g) > G (4.5 g) > A (4.4 g) > E (4.2 g) > H (3.8 g) > K (3.7 g) > I (3.5 g) > B (3.0 g)

Examples of recorded results by the hot plate test

The scatter of the ignition delay times was very large. The examples of original data are listed in Table 4. Large scatters in the test may come from the exceptional extremely short delay time, which in turn may come from the quick ignition of the small powdery fragments or a sharp edge of the sample. Smaller particles are easier to ignite than larger pieces. Because of the large scatter, log τ was used instead of ignition delay time τ for statistical treatment.

The standard deviation of log τ of the primer D was lowest among the tested samples, because there was no exceptionally short ignition delay time. That of the burst charge 3 was largest, because of the existence of exceptionally short and long τ. The piece of the burst charge was more easily fragmented than the pieces of the other samples. In the case of the yellow star, there was an exceptionally short τ, probably owing to the broken small fragments.

Table 3 *Ignition limit lift charge of bare and primed stars.*

	Ignition limit lift charge/g					
	Red	Green	Blue	Yellow	Purple	Mean
Bare star	0.15	0.30	0.30	0.50	0.50	0.35
Primed star						
Prime A	3.50	4.50	6.50	2.50	5.00	4.40
Prime B	2.00	0.65	5.00	4.50	3.00	3.00
Prime C	1.50	7.00	6.00	4.00	5.00	4.70
Prime D	4.50	5.50	6.00	3.00	5.00	4.80
Prime E	3.00	4.00	5.00	2.00	7.00	4.20
Prime F	2.00	3.50	8.50	6.00	7.00	5.50
Prime G	4.00	4.50	4.50	7.00	2.50	4.50
Prime H	3.50	4.00	3.00	4.00	3.00	3.80
Prime I	2.50	3.50	3.50	4.50	3.50	3.50
Prime J	4.50	3.50	6.00	6.00	4.50	4.90
Prime K	0.75	2.50	7.00	6.00	2.00	3.70
Prime L	6.00	4.50	3.50	4.50	4.50	4.60
Mean	3.10	4.00	5.40	4.50	4.30	4.30

Reproducibility of the hot plate test results

The mean and standard deviation (SD) of log τ of piece samples at 700 ºC and 600 ºC are listed in Table 5.

At first the experiments for the hot plate test were conducted at 700 ºC. Then the experiments were carried out at different temperatures from 600 ºC to 800 ºC and the lowest standard deviations of log τ were obtained at 600 ºC. But at 600 ºC, values of log τ for star compositions were not necessarily larger than those for other compositions.

The mean and SD of log τ at different temperatures are listed in Table 6, and the plot of SD against the reciprocal is temperature shown in Figure 6.

Results of the electric match test

The electric match test was applied to the pieces of prime A–D, lift and burst charges, and star compositions. The results are listed in Table 7. The probability of ignition in this test was lowest for green star composition and highest for prime C and D compositions. This method may be used for differentiating the ignitability of star and prime compositions.

Correlation of the hot plate and electric match tests results

The plot of log τ at 700 ºC in the hot plate test against the ignition probability in the electric match test is shown in Figure 7. The primes C and D have the highest ignitability by this test among primes A–G. However, these results do not necessarily agree with those of the shot test results, probably because there is some scatter of the data in the results of the electric match test.

Correlation of the hot plate and electric match tests results with the shot test results

The plots of log τ at 700 ºC in the hot plate test and the ignition probability in the electric match test against the ignition limit lift charge in the shot test are shown in Figure 8. It is found from Figure 7 that there is a large difference between the ignition limit lift charges of bare stars and primed stars tested. There are positive and negative correlations between the ignition limit lift charge, and the

Table 4. *Examples of observed results at 700 ºC.*

Sample	Drop time/ms	Ignition time/ms	Delay time τ/ms	log τ
	3120	3700	580	2.76
	3230	3955	725	2.86
Primed D	2777	3537	760	2.88
	2455	3044	589	2.77
	2705	3387	682	2.83
Mean			667	2.82
SD[a]			81	0.05
RSD[b]			0.12	
	10870	10970	100	2.00
	10985	11725	740	2.87
Lift charge	10880	11532	652	2.81
	10617	10912	295	2.47
	10437	10652	215	2.33
Mean			400	2.50
SD[a]			280	0.36
RSD[b]			0.70	
	11172	11192	20	1.30
	10720	10952	232	2.37
Burst charge 3	10687	10742	55	1.74
	10610	12452	1842	3.27
	11005	11147	142	2.15
Mean			458	2.16
SD[a]			778	0.74
RSD[b]			1.70	
	11507	13940	2433	3.39
	10445	12957	2512	3.40
Yellow bare star	10607	11057	450	2.65
	10417	12252	1835	3.26
	10732	13202	2465	3.39
Mean			1939	3.22
SD[a]			877	0.32
RSD[b]			0.45	

[a] Standard deviation. [b] Relative standard deviation (SD/mean).

ignition probability in the electric match test and log τ at 700 ºC in the hot plate test, respectively. It seems that the shot test is the best ignitability test among the three test methods, and the other two methods may be used as screening methods.

Conclusion

Table 5. *Mean and standard deviation (SD) of log τ.*

Sample	T/ºC	Mean of log τ	SD of log τ
Prime A	700	2.57	0.13
	600	3.55	0.08
Prime B	700	2.31	0.45
	600	3.35	0.24
Prime C	700	2.75	0.21
	600	3.64	0.28
Prime D	700	2.82	0.05
	600	3.31	0.15
Prime E	700	3.02	0.08
	600	3.56	0.09
Prime F	700	2.73	0.27
	600	3.46	0.12
Prime G	700	2.89	0.21
	600	3.56	0.08
Prime H	700	3.19	0.18
Prime I	700	2.71	0.46
Prime J	700	2.45	0.54
Prime K	700	2.54	0.52
Prime L	700	2.62	0.36
Lift charge	700	2.50	0.36
	600	3.40	0.08
Burst charge 3A[a]	700	2.16	0.74
	600	3.44	0.42
Burst charge 3B[a]	700	2.61	0.25
Burst charge 5A[a]	700	2.58	0.41
Burst charge 5B[a]	700	2.53	0.41
Burst charge SA[a]	700	2.55	0.41
Burst charge SB[a]	700	3.01	0.22
Yellow star	700	3.22	0.32
	600	3.78	0.08
Red star	700	3.35	0.32
	600	3.72	0.08
Green star	700	3.32	0.10
	600	3.91	0.14
Blue star	700	3.00	0.26
	600	3.36	0.12
Purple star	700	3.27	0.16
	600	3.03	0.06

[a] Burst charge 3A and 3B are the piece and original grain burst charges, respectively, for no. 3 shell. S stands for special shells.

Table 6. *Temperature, reciprocal temperature, and mean and SD of log τ of samples.*

Sample	T/ºC	$1000/T$ (K^{-1})	Mean of log (τ/ms)	SD of log τ
	600	1.145	3.31	0.15
	650	1.083	3.31	0.14
Prime D	700	1.028	2.82	0.05
	750	0.978	2.63	0.40
	800	0.932	2.63	0.40
	600	1.145	3.40	0.08
	650	1.083	3.24	0.19
Lift charge	700	1.028	2.50	0.36
	750	0.978	2.28	0.15
	800	0.932	2.54	0.32
	600	1.145	3.78	0.08
	650	1.083	3.75	0.11
Yellow star	700	1.028	3.22	0.32
	750	0.978	3.00	0.19
	800	0.932	3.08	0.28

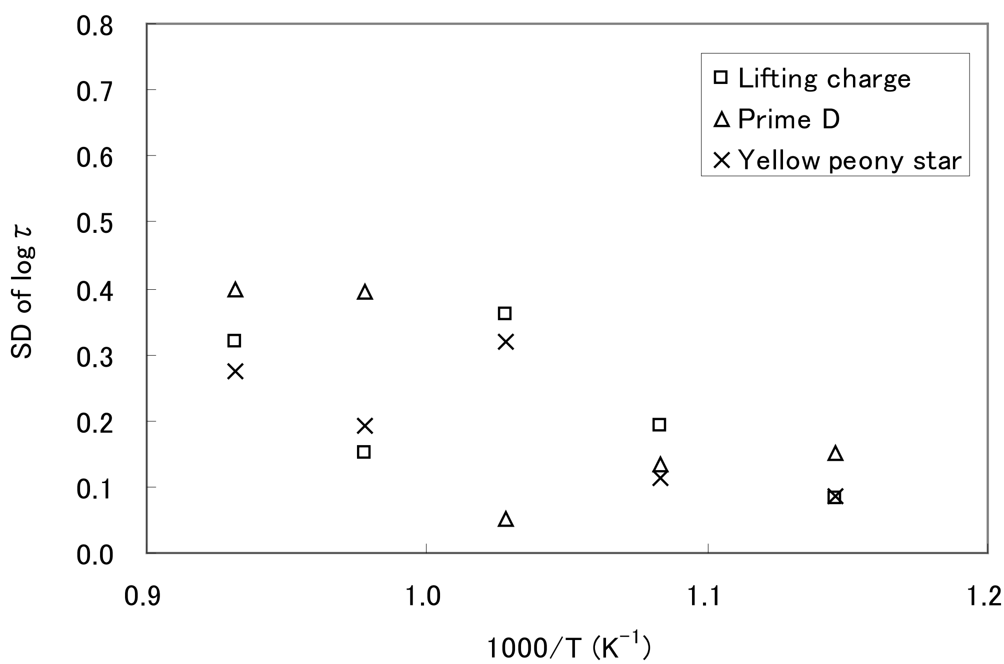

Figure 6. *Plot of SD of log τ vs. 1000/T.*

Table 7. *Results of electric match test.*

Sample	Ignitions/Trials
Prime A	8/10
Prime B	7/10
Prime C	10/10
Prime D	10/10
Prime E	9/10
Prime F	8/10
Prime G	8/10
Lift charge	8/10
Burst charge	9/10
Star red	4/10
Star green	0/10
Star yellow	7/10
Star blue	6/10
Star purple	5/10

The shot test was applied to the ignitability of bare and primed stars, and was found to be a useful method for evaluating the ignitability of the stars though there was some scatter in the observed data. The hot plate and electric match tests were applied to the ignitability of prime, star, lift and burst charge compositions. The hot plate and electric match tests may be used for screening the ignitability of the firework compositions.

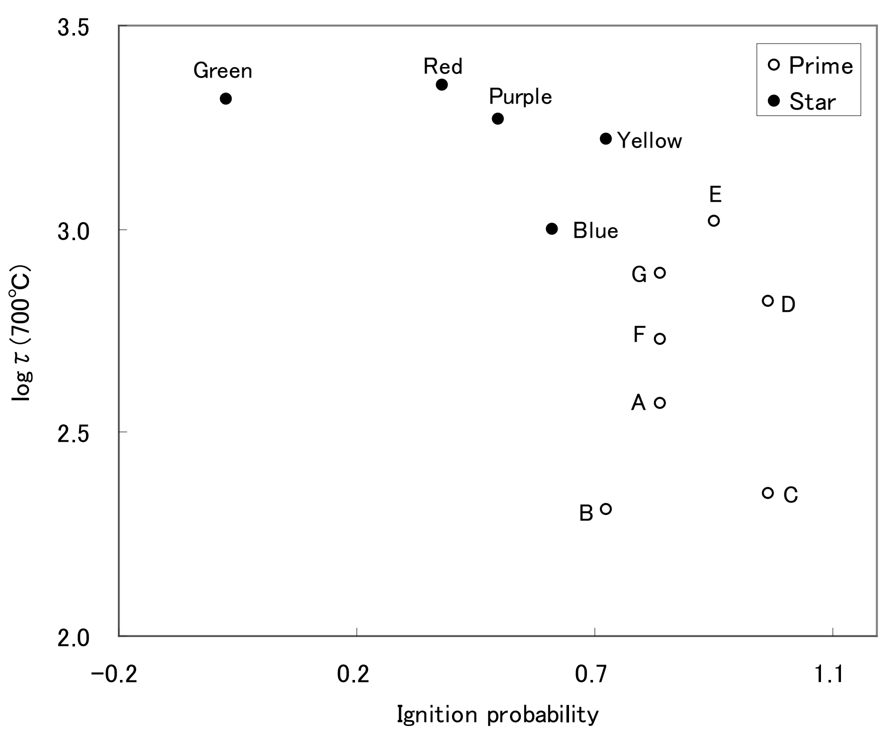

Figure 7. *Plot of log τ (at 700 °C) in hot plate test vs. ignition probability in electric match test.*

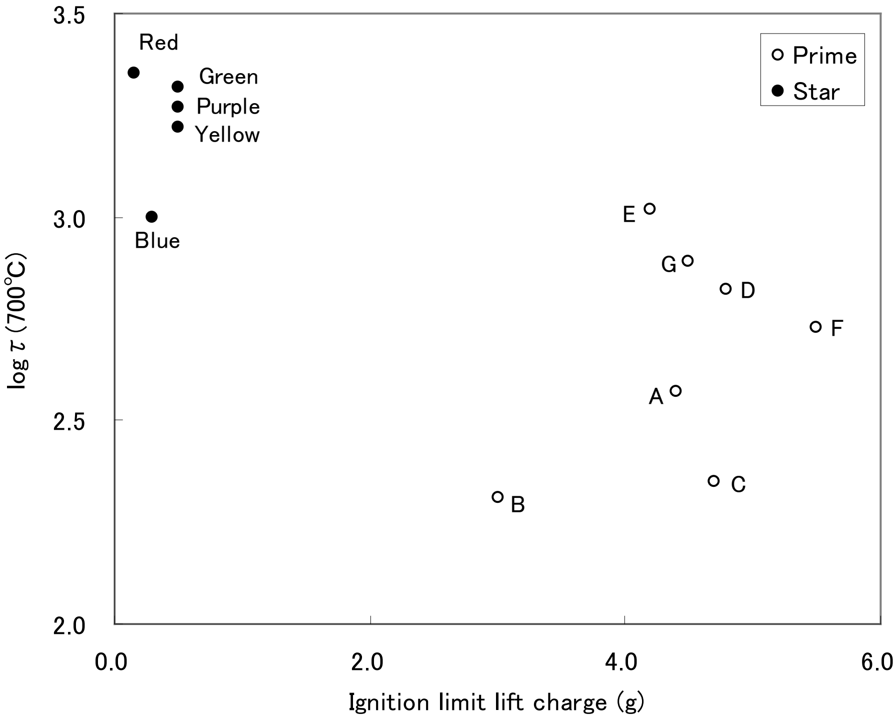

Figure 8. *Plots of log τ (at 700 ºC) and ignition probability vs. ignition limit lift charge for bare and primed stars.*

References

1 T. Yoshida, *Safety of Reactive Chemicals*, Elsevier, 1987.

2 T. Yoshida, Y. Wada and N. Foster, *Safety of Reactive Chemicals and Pyrotechnics*, Elsevier, 1995.

3 H. Keonen, K. I. Ide and K. H. Swart, "Sicherheitstechnische Kensaten Explosionstahlgen Stoffe", *Explosivestoffe*, vol. 9, 4 and 30, 1961.

4 Japan Explosive Society, *Test Manual for Explosives. ES-11*, 1996, pp. 1–2.

5 K. L. Kosanke and B. J. Kosanke, "Pyrotechnic Primes and Priming", in *Pyrotechnic Chemistry*", ed. K. L. Kosanke and B. J. Kosanke, ch. 7, Journal of Pyrotechnics, Inc., 2004.

6 Y. Sashimura, M. Horiuti, H. Watanabe, M. Watanabe, D. Ding and T. Yoshida, "Ignitability of Cylindrical Firework Stars", *Science and Technology of Energetic Materials*, in contribution.

7 *Manufacture and Safety of Fireworks,* All Japan Association for Safety of Explosives, 2006, p. 96.

Spectroscopic Measurement of Burning Toy Fireworks

Kazuomi Itoh, Dayu Ding and Tadao Yoshida*
Ashikaga Institute of Technology
286-1 Omae-cho, Ashikaga-shi, Tochigi 326-8558, Japan
Tel: +81-284-62-0605, fax: +81-284-62-0976, email: yoshida@ashitech.ac.jp
*To whom all correspondence should be addressed.

Abstract: *The spectroscopic measurement of sparklers, torches and senko hanabi (Japanese sparklers) was carried out. The three dimensional spectra of sparklers and torches showed that the peak intensities of the spectra fluctuate with time. In the burning of sparklers, white, titanium, senko and iron sparklers showed mainly the K peak suggesting that the incandescent emission is principally in the visible light area. The white and titanium sparklers showed high K peak intensities compared to other sparklers suggesting the high temperature burning of Al and Ti. Among the tested sparklers the excitation purities of titanium and blue sparklers were relatively low. Regarding torches, the flame, sparks and falls were compared. The K peak intensity of falls was largest compared to other kinds of torches, presumably because the falls contain the energetic aluminum. The purity of the blue torch was exceptionally small. The spectra and photographs of burning sparklers and torches were compared. The fireball and the branching sparks of senko hanabi were recorded using the profiles of K peak intensity of the senko hanabi at two burning locations.*

Keywords: *toy fireworks, spectroscopic measurement, emission spectra, torch, sparkler, glitter, senko hanabi*

Introduction

Light emission, beautiful colors and glittering sparks are important effects in toy fireworks. Sparklers, torches and senko hanabi are typical toy fireworks in Japan.

In the present work, spectroscopic measurements were carried out in order to study the spectra and burning characteristics of sparklers, torches and a senko hanabi toy firework.

Experimental

Materials

The toy fireworks used in this work were supplied by Inoue Toy Fireworks Co. Ltd. The Color Change Five Mix 5P is a set of five torches, in which the flame colors each change twice. The Color Change Torch Pro 10 Colors has flame and spark colors that change ten times. The Eight Spark 8P are eight sparklers containing red, green, yellow and blue flames, senko, titanium, iron and aluminum glitters. The senko hanabi is a Japanese traditional toy firework and produces glitter. The toy fireworks used are shown in Figure 1.

Apparatus

The spectrometer PMA-11C7473-36 is a product of Hamamatu Photonics Co. Ltd. The spectrometer is composed of an optical fiber for light intake, photo detector, spectroscope, basic software and data analyzer. The analyzer automatically calculates and records the spectrum, the respective peak wavelength and intensity, the excitation

Figure 1. Toy fireworks used in this work.

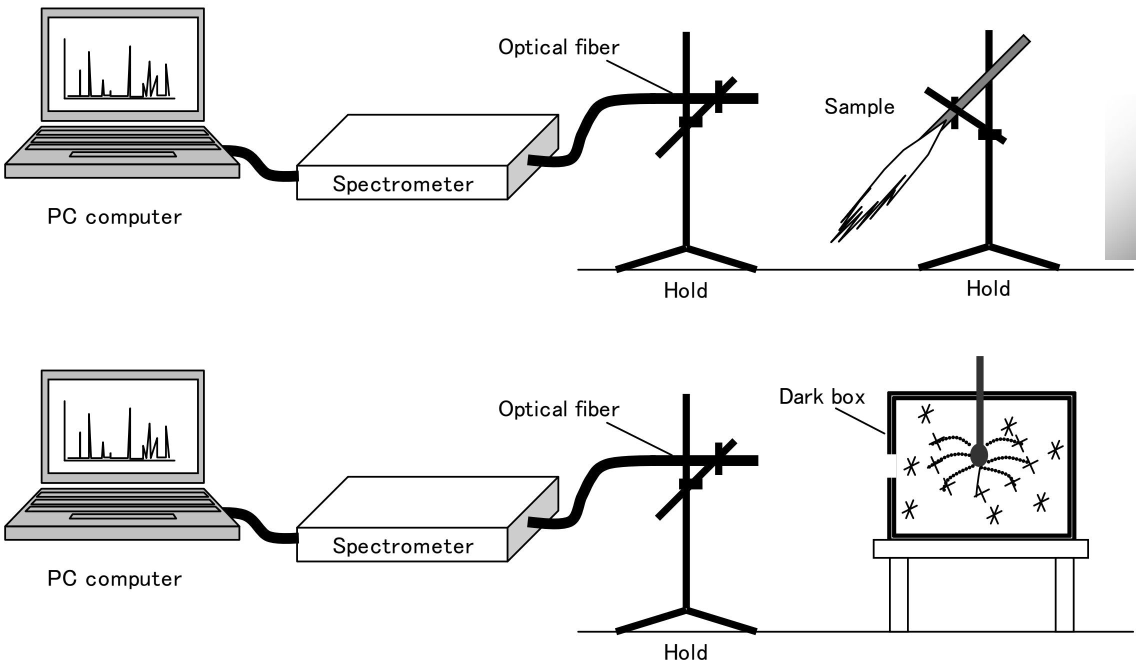

Figure 2. *Setup of the spectroscopic measurement of burning toy fireworks: sparkler and torch (upper) and senko hanabi (lower).*

purity, and so on.

The spectrometer is equipped with following functions: exposure time from 20 ms to 32 767 ms, averaging repetition from 1 to 32 767, exposure repetition from 1 to 32 767, and sensitivity low or high. The background noise can be compensated by adjusting the bias current to establish a zero baseline.

The analyzers can print out the emission spectrum at a specified time, the peak intensity profile at a specified wavelength and the three dimensional picture of the spectrum with time.

Procedure

The setup of the samples is shown in Figure 2. A torch or sparkler is supported by a clamp stand in a draft chamber and ignited by a torch burner. A senko hanabi is suspended vertically from the lid of a dark box, and ignited by a torch burner. The tip of the optical fiber of the spectrometer is placed at 4 m from the torches and sparklers and at 0.18 m from the senko hanabi.

The power sources of the spectrometer and the PC are switched on successively. The measurement conditions such as instrument sensitivity, exposure time, averaging repetition numbers, and observation repetition are set and the dark electric current is compensated. The spectrometer measurement is started at the point of ignition of the firework.

Results and Discussion

Fluctuation of the emission intensity of the sparklers and torches

The flames of firework sparklers and torches look rather uniform against time to the eye. However, the three dimensional spectra shown in Figure 3 indicate that the intensities of the spectral peaks fluctuate with time. The firework compositions are mixtures of solid particles and the combustion of the mixtures may be not uniform.

Spectra of burning sparklers

Figure 4 shows the spectra of burning sparklers. The following assignment of each peak was done according to Meyerriecks and Kosanke.[1] The yellow sparkler has three main peaks: the highest peak is assigned to K (766 nm), the second to Na (589 nm) and the third to CaCl (618 nm). The excitation purity was 72%. The green sparkler has five main peaks: the highest is assigned to K

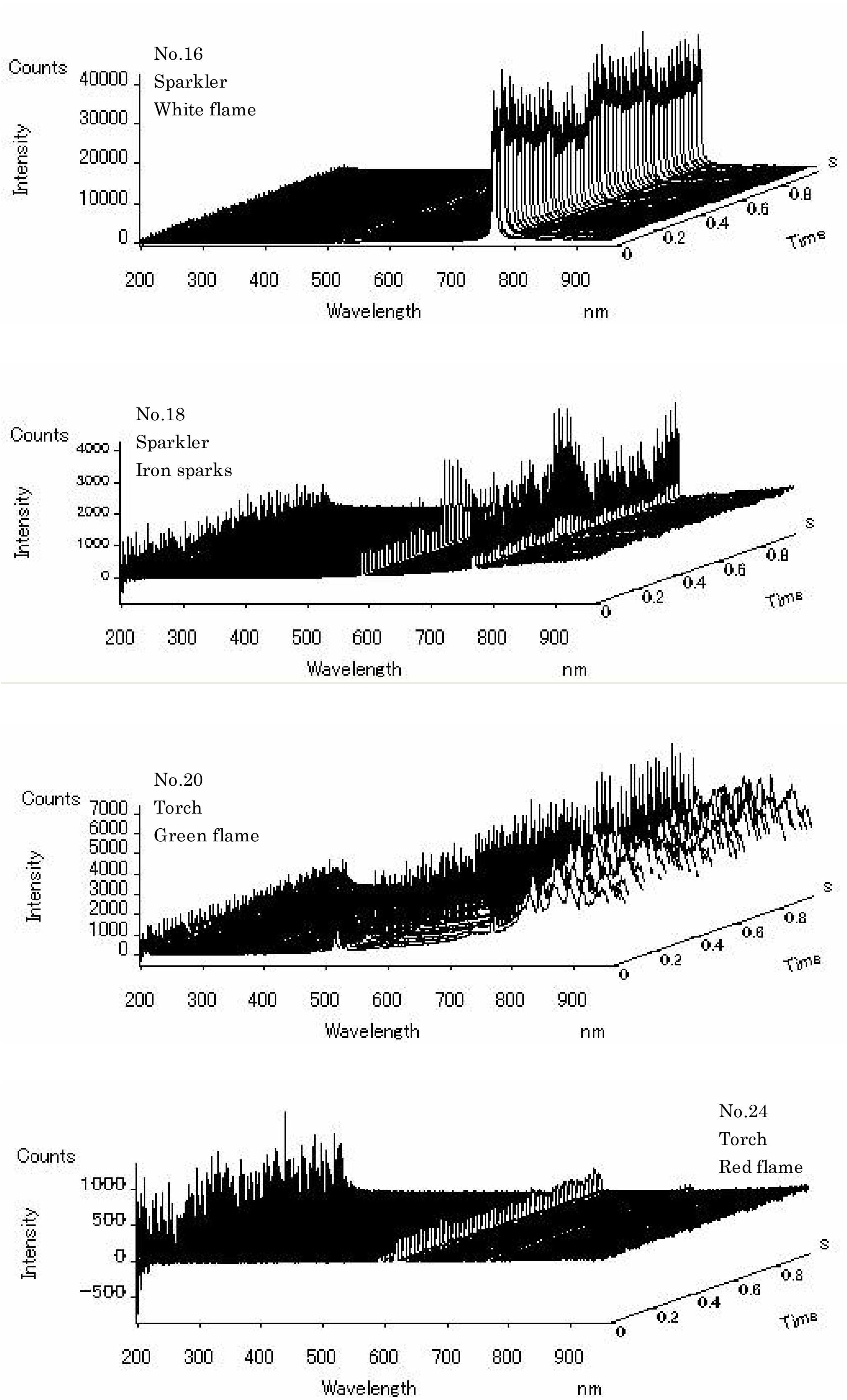

Figure 3. *Three dimensional spectra of burning sparklers and torches.*

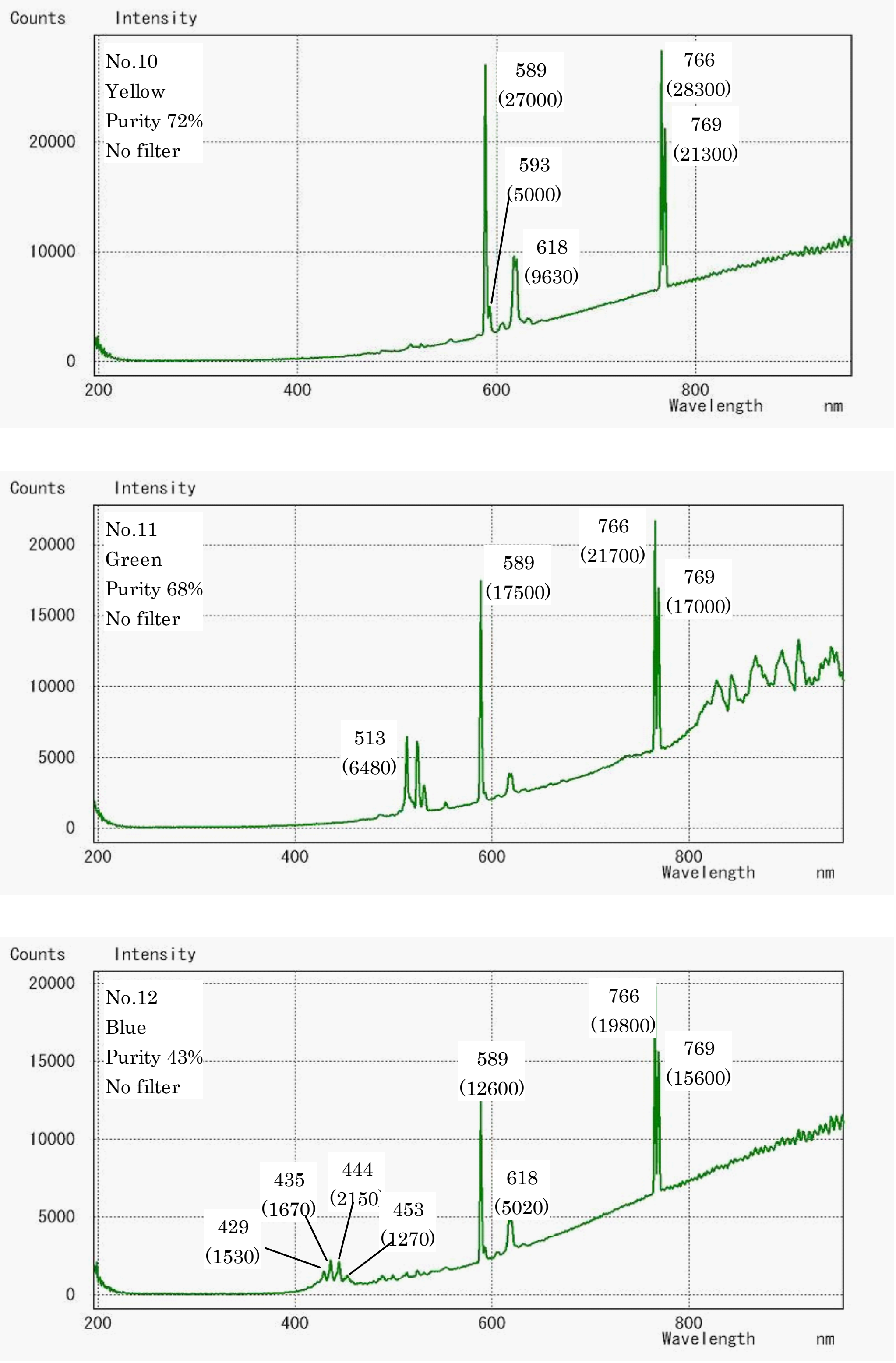

Figure 4. *Spectra of burning firework sparklers.*

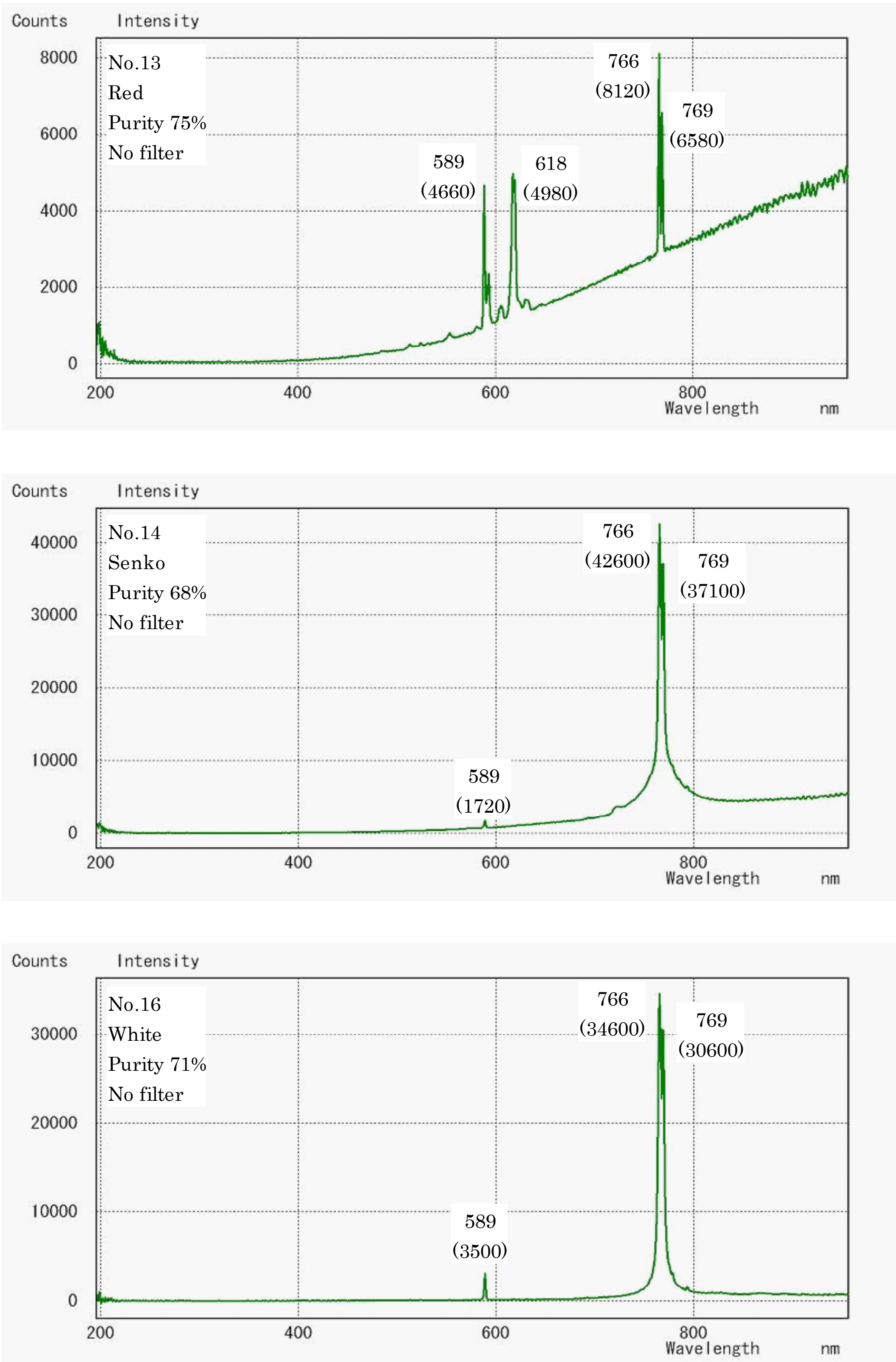

Figure 4 (contd). *Spectra of burning firework sparklers.*

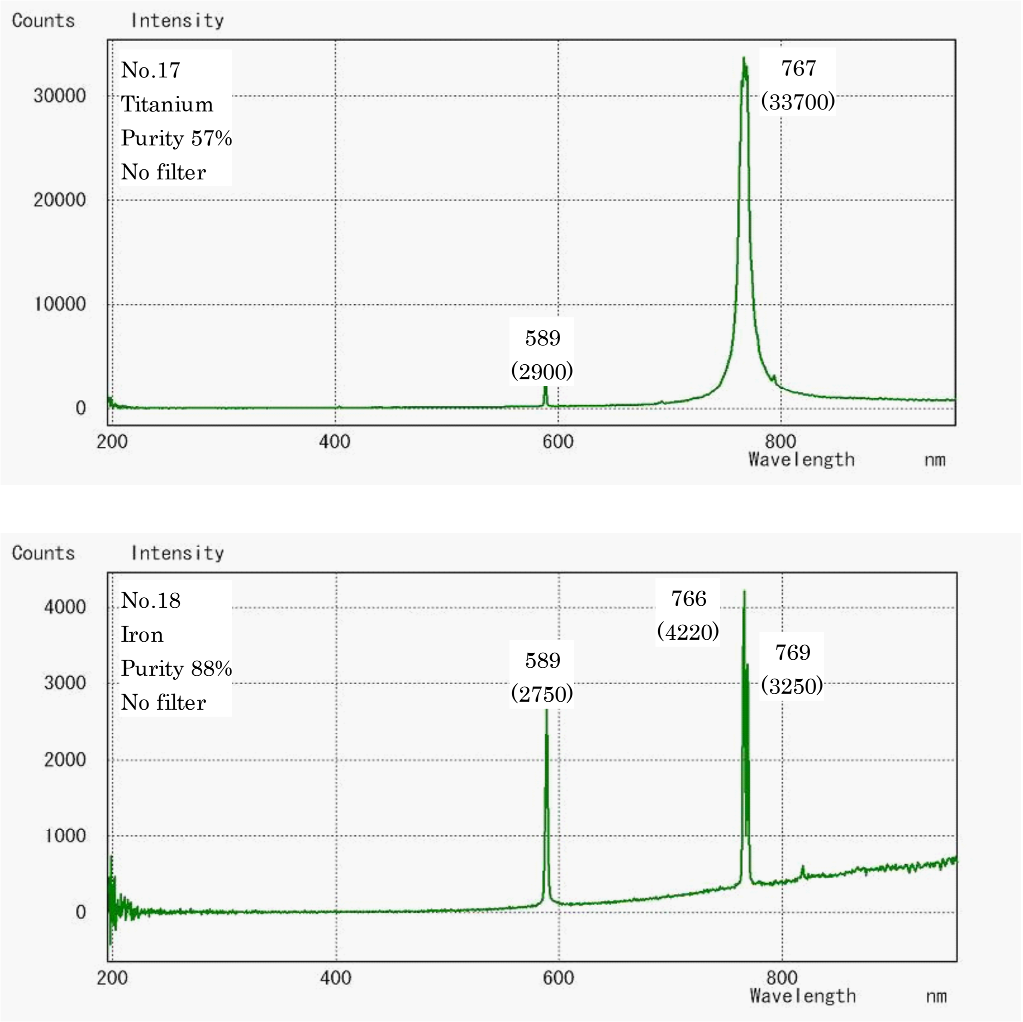

Figure 4 (contd). *Spectra of burning firework sparklers.*

(766 nm), the second to Na (589 nm), the third to an unidentified band spectrum (800–900 nm), the fourth to BaCl (513 nm) and the fifth to CaCl (618 nm). The blue sparkler has four main peaks assigned to K (766 nm), Na (589 nm), CaCl (618 nm) and CuCl (444 nm). The red sparkler has three main peak groups assigned to K (766 nm), CaCl (618 nm) and Na (589 nm). The senko, white and titanium sparklers have only one main peak assigned to K (766 nm) and the iron sparkler has two main peaks assigned to K (766 nm) and Na (589 nm). All spectra may contain incandescent emissions in the rising base lines.

The highest K peaks in the infrared emitters and the species in visible color emitters, and the exciting purities of sparklers are listed in Table 1.

Spectra of burning torches

The spectra of the burning torches are shown in Figure 5. The spectra of the green flame (No. 20), sparks (No. 38) and falls (No. 37) were recorded. All green spectra are composed of K, Na, BaCl and unidentified peaks which may be assigned to a Ba compound. The peak intensities and the excitation purities of three green torches, and the ratios of peak intensities in the three torches were different. Regarding the intensities of the BaCl green peak the order corrected to no filter was as follows: falls (120 000 counts) > sparks (5900 counts) > flame (3600 counts). The ratio of peak intensities of BaCl and Na was as follows: falls (2.19) > sparks (1.11) > flame (0.81). The excitation purity was: sparks (68%) > flame (64%) > falls (56%).

Table 1. *Important peaks in the spectra of burning sparklers.*

Sparklers	Species	Intensity (counts)	Excitation purity (%)
Yellow	K	2.83×10^4	72
	Na	2.70×10^4	
Green	K	2.17×10^4	68
	BaCl	6.47×10^3	
Blue	K	1.98×10^4	43
	CuCl	2.15×10^3	
Red	K	8.12×10^3	75
	CaCl	4.98×10^3	
Senko	K	4.26×10^4	68
	Na	1.72×10^3	
White	K	3.46×10^4	71
	Na	3.50×10^3	
Titanium	K	3.37×10^4	57
	Na	2.90×10^3	
Iron	K	4.22×10^3	88
	Na	2.75×10^3	

The reason for the differences are not clear at the moment, but the highest intensity of the green falls may be ascribed to the high content of aluminum in the fall composition and the highest combustion temperature.

The spectra of the red flame (No. 24) and sparks (No. 29) were composed of peaks of CaCl (618 nm), K (766 nm) and a little Na (589 nm). The peak intensity (750 counts) of CaCl in the sparks was larger than that (420 counts) in the flame, and the ratio (3.20) of the peak intensities of CaCl to K was higher in the flame than that (0.92) in the sparks presumably because the amount of potassium perchlorate was smaller in the red flame (No. 24) than in the red sparks (No. 29). The excitation purity (87%) of the flame was higher than that (75%) of the sparks.

No. 36 and No. 39 are the spectra of red sparks and fall torches using SrCl (672 nm) as a red emitter. The peak intensity (4200 counts) of SrCl in the falls was larger than that (860 counts) in the sparks. The excitation purities of the sparks and falls were 58% and 60%, respectively, and lower than those using CaCl as red color emitter.

No. 34 and No. 26 are the spectra of the yellow sparks and fall torches. The main peaks were Na (589 nm) and K (766 nm). The intensity (14 000 counts) of the Na peak in the falls was much larger than that (1400 counts) in the sparks. The ratio (3.68) of the Na to K peaks in the sparks was much higher than that (0.34) in the falls. On the other hand, the excitation purity (86%) of the falls was greater that (68%) in the sparks. This is the opposite of the case of the green torch.

No. 35 is the spectrum of the blue torch falls composed of CuCl (444 nm), BaCl (513 nm), Na (766 nm), K (766 nm) and an unidentified infrared emitter. An extremely low excitation purity was observed.

No. 23 and No. 30 are the purple flame and fall torches. The spectra of both fireworks were composed of those of CuCl, BaCl, Na, CaCl and K. The peak intensity (1200 counts) of CaCl in the falls was higher than that (290 counts) in the flame. The ratio (0.74) of CuCl to CaCl peak intensities in the flame was greater than that (0.18) in the falls. The excitation purities were 38% and 23% in the flame and falls, respectively.

A summary of the results is listed in Table 2. Generally, the peak intensities of falls, sparks and flame were in following order:

falls > sparks > flame

The reason for the order may be the higher Al or Ti content in the falls than in the sparks, and the absence of such metals in the flames.

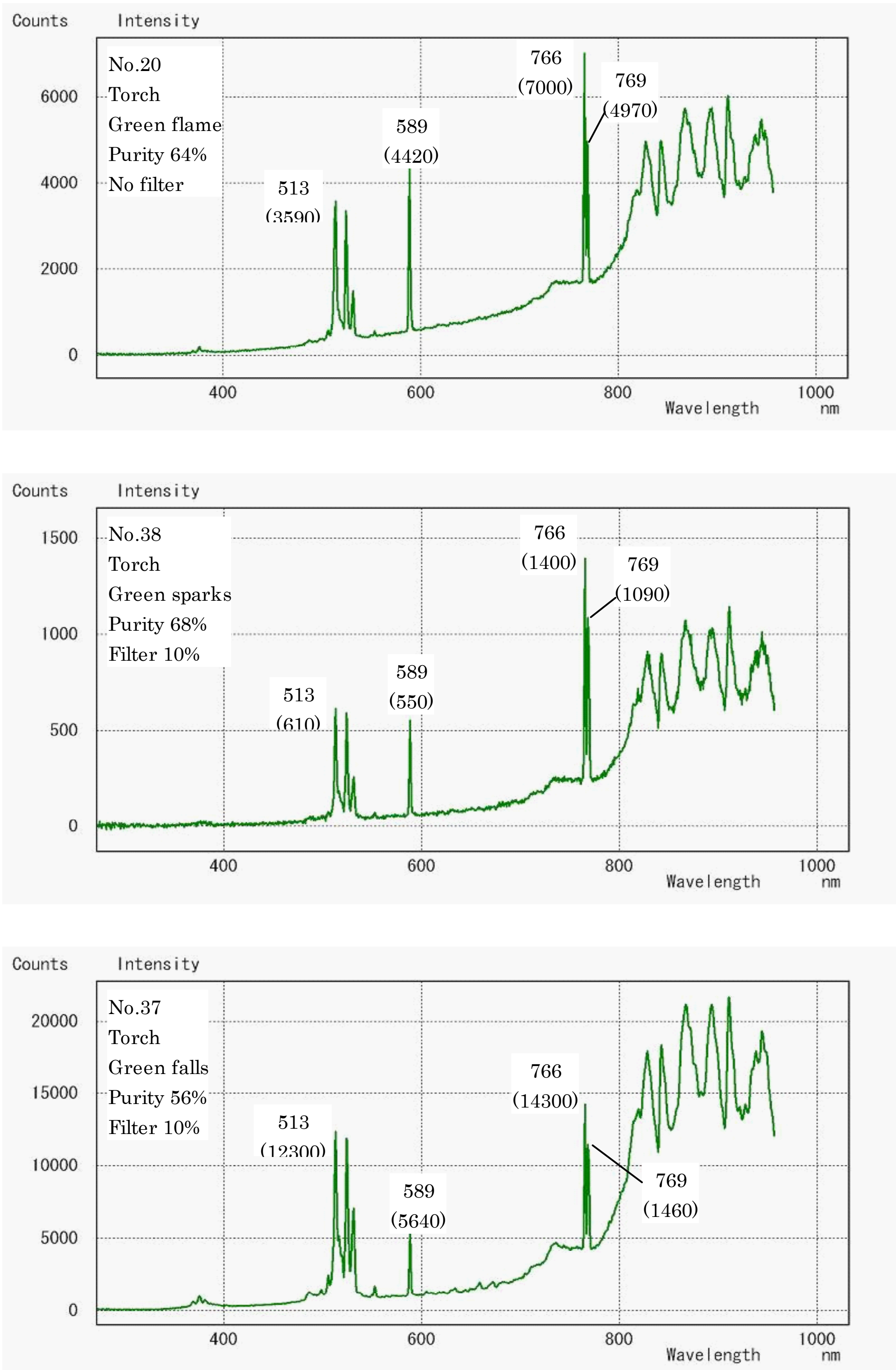

Figure 5. *Spectra of burning torches.*

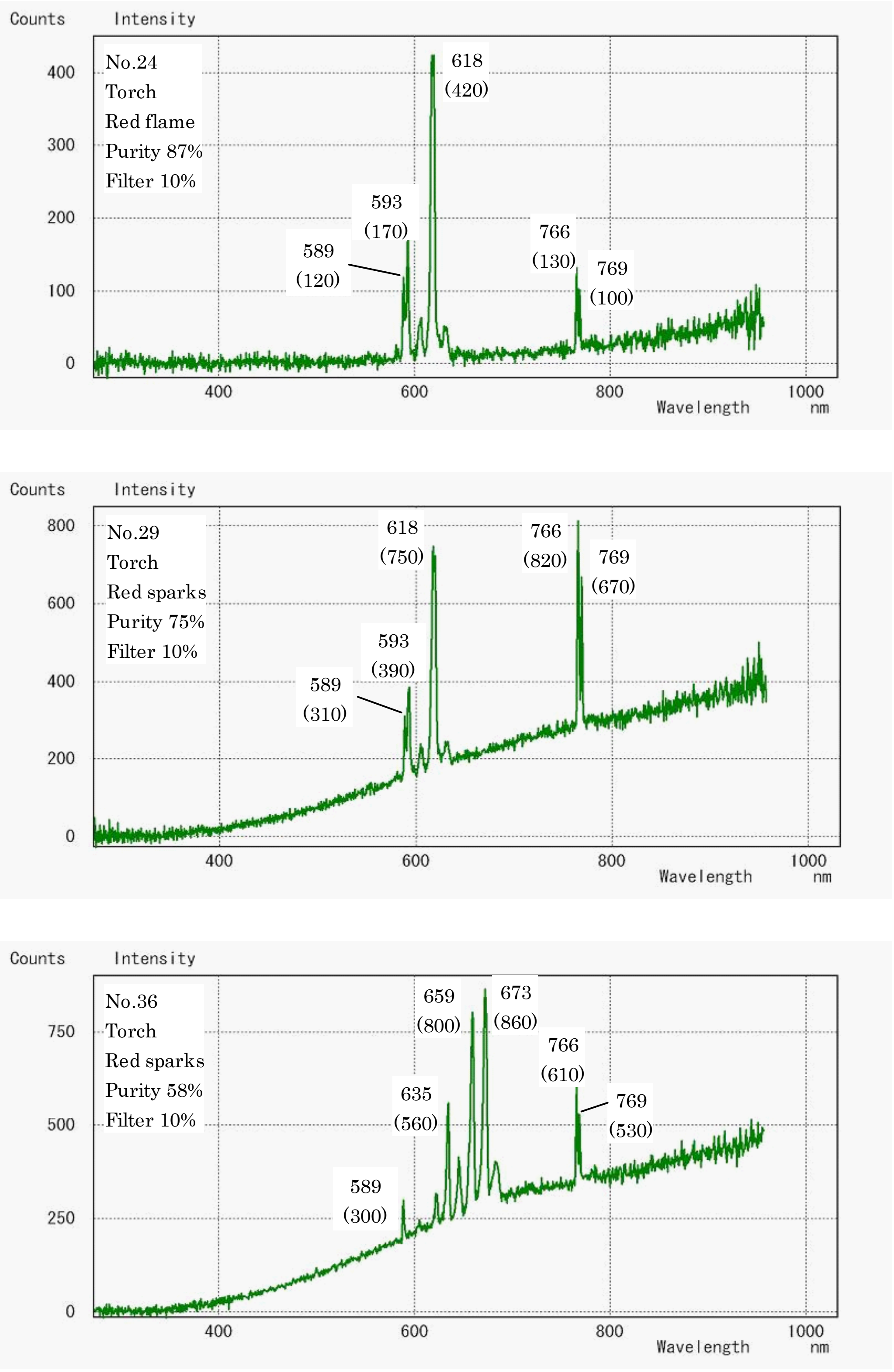

Figure 5 (contd). *Spectra of burning torches.*

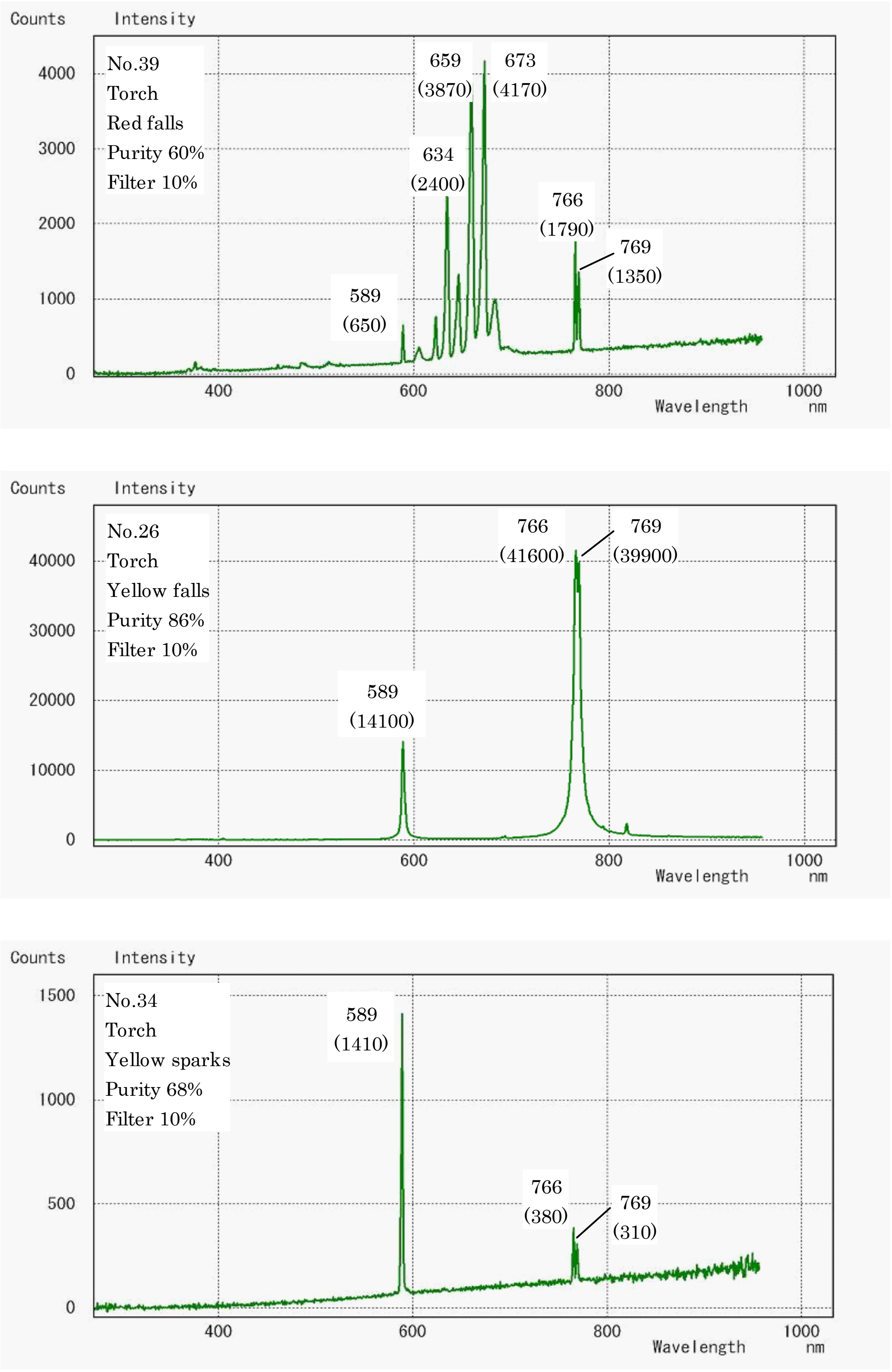

Figure 5 (contd). *Spectra of burning torches.*

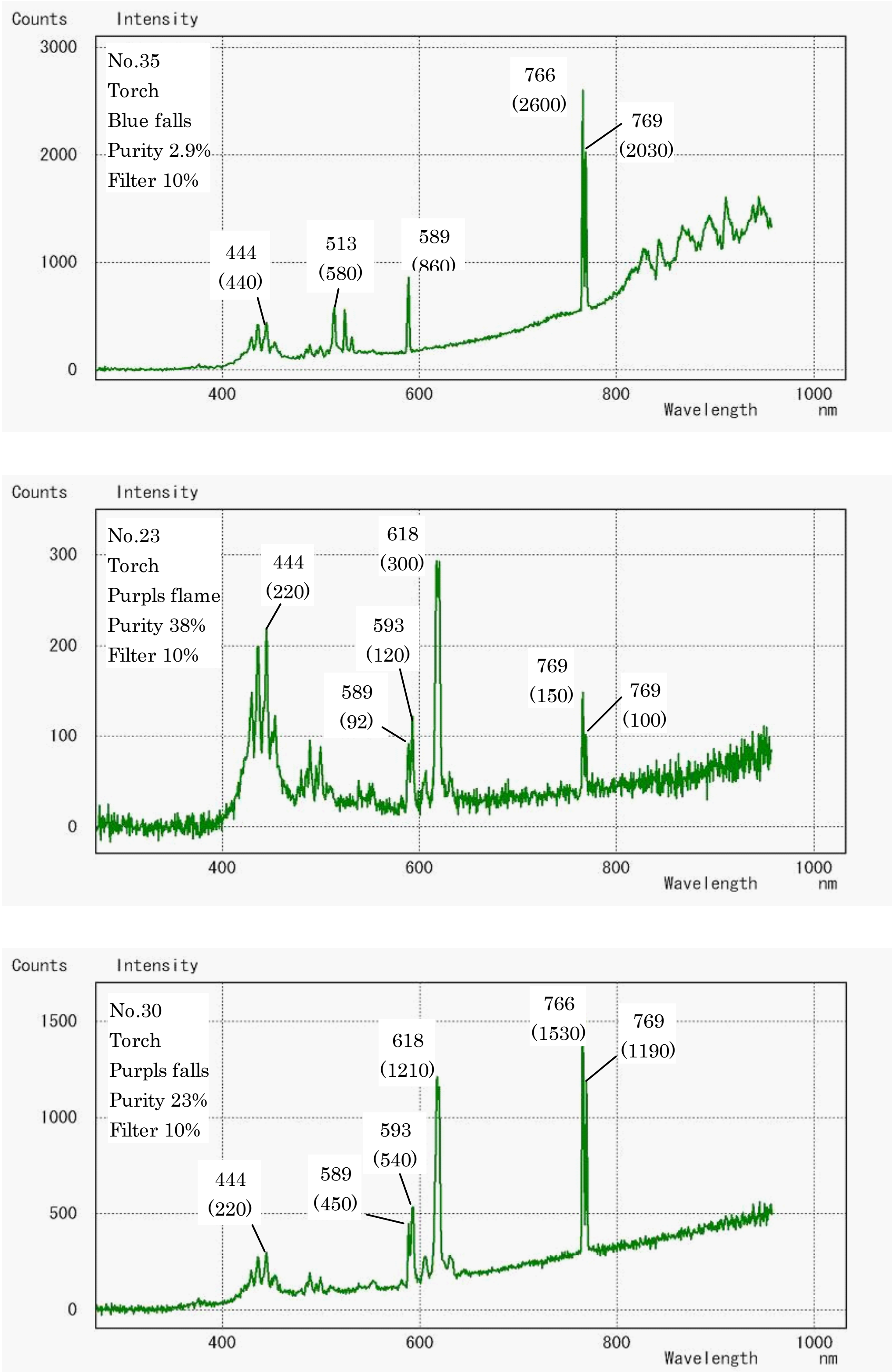

Figure 5 (contd). *Spectra of burning torches.*

Table 2. *Summary of the spectroscopic measurement of the burning sparklers and torches.*

No.	Color	Kind	Emitter (counts)				Purity (%)
13	Red	Sparkler	Na (4700),	CaCl (5000),	K (8100)		75
24	Red	Torch flame	Na (1700),	CaCl (4200),	K (1300)		87
29	Red	Torch sparks	Na (3100),	CaCl (7500),	K (8200)		75
36	Red	Torch sparks	Na (3000),	SrCl (8600),	K (6100)		58
39	Red	Torch falls	Na(6500),	SrCl (42000),	K (18000)		60
10	Yellow	Sparkler	Na (27000),	CaCl (9600),	K (28000)		72
34	Yellow	Torch sparks	Na (14000),		K (3800)		68
26	Yellow	Torch falls	Na (140000),		K (420000)		86
11	Green	Sparkler	BaCl (6500),	Na (17000),	K (22000)		68
20	Green	Torch sparks	BaCl (44000),	Na (44000),	K (70000)		64
38	Green	Torch sparks	BaCl (5900),	Na (5520),	K (14000)		68
37	Green	Torch falls	BaCl (120000),	Na(5600),	K(140000)		56
12	Blue	Sparkler	CuCl (2200),	Na (13000),	K (20000)		43
35	Blue	Torch falls	CuCl (4400),	BaCl (5800),	Na (8600),	K (2600)	2.9
23	Purple	Torch flame	CuCl (2200),	Na (920),	CaCl (2900),	K (1500)	38
30	Purple	Torch falls	CuCl (2200),	Na (4500),	CaCl (12000),	K (15000)	23

The senko hanabi gives the so called "fire-branching sparks". The phenomenon of senko hanabi was described by Shimizu as follows:[2] When it is ignited, it burns violently with a flame at first, then the remaining ash keeping its red-hot state, contracts itself to a small red-hot ball, which is the so-called "fireball". After a few seconds, the temperature of the fireball gradually rises and fine particles begin to fly out of the ball. The particles become more brilliant at a short distance from the ball and explosively branch into fine needle-like sparks.

Figure 6 shows a spectrum of the center of a burning senko hanabi. The spectrum has a single K peak in the infrared region. The visible light of senko hanabi comes from the incandescent emission of the condensed phase products. Figure 7 shows the change of the K peak intensity with time in the same experiment. When the senko hanabi was ignited, a strong peak intensity

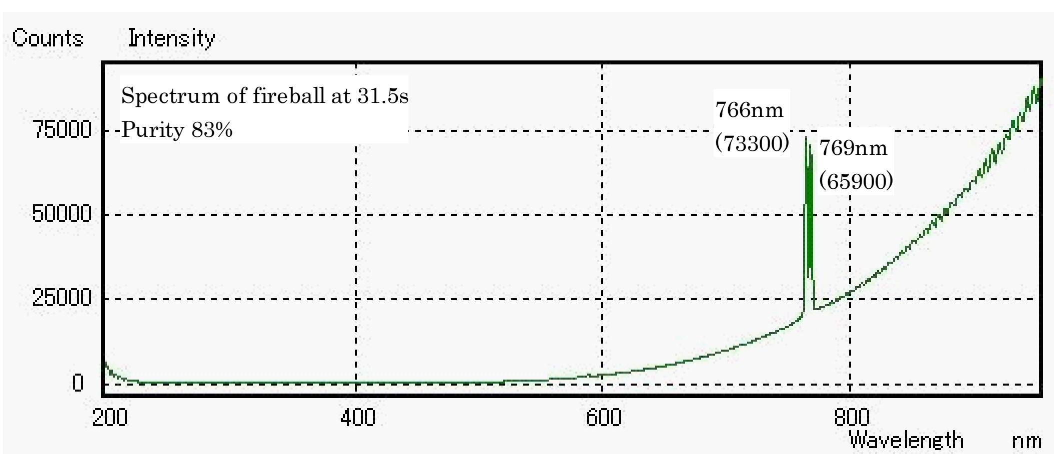

Figure 6. *Spectrum at the center of burning senko hanabi.*

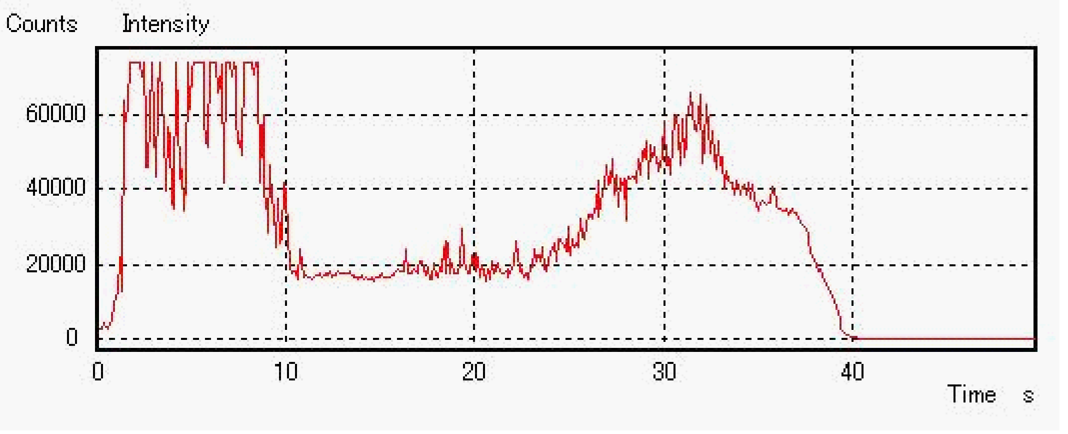

Figure 7. *766 nm peak intensity profile at the center of burning senko hanabi.*

continued corresponding to the initial violent burning of the senko hanabi. Then the intensity of the peak decreased to a lower level, and after few seconds, the intensity increased corresponding to the formation of a growing fireball. The emission from the fireball increased and peaks appeared intermittently, corresponding to the fire-branching sparks.

Figure 8 shows a spectrum of the center of the fireball with fire-branching sparks at 30.7 s. Figure 9 shows the K peak intensity change with time during the burning of a senko hanabi. In this case, the direction of the optical fiber of the spectrometer was aimed at the area around the fireball, in order to catch only the branching sparks avoiding the fireball. At first, the peak from the initial flame appeared, then after few seconds intermittent fine peaks appeared without the broad peaks of the fireball. The fine peaks might come from the emission of the sparks only. The intensity of the emission of the senko hanabi was lower than that of other toy fireworks such as sparklers and torches. Therefore the senko hanabi is enjoyed from a short distance by children.

The spectra of the fireball and sparks of a senko hanabi are very similar as shown in Figure 6 and Figure 8. In the spectra of the fireball and sparks of a senko hanabi only two K peaks appear, and the excitation purities were 83% and 85%, respectively.

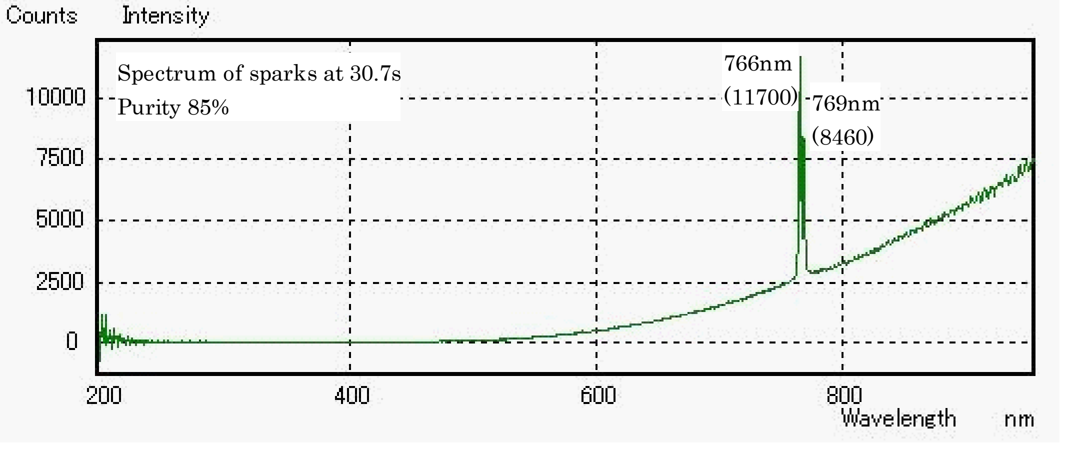

Figure 8. *Spectrum of the sparks in the neighborhood of a senko hanabi fireball.*

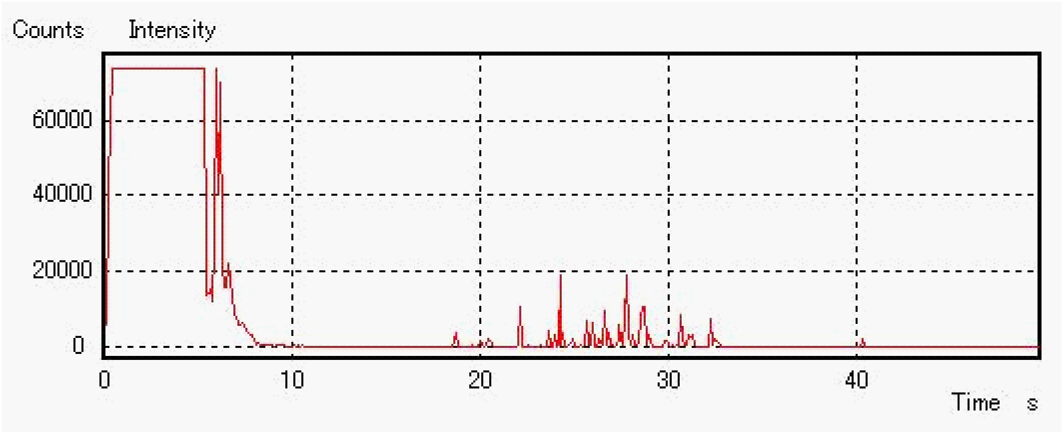

Figure 9. *766 nm peak intensity profile at neighborhood of fireball of senko hanabi.*

The orange color of the fireball and sparks of the senko hanabi comes from the incandescent emission of the condensed phase of the fireball and the sparks. The rising base lines of the spectra from 600 nm may be attributable to the incandescent emissions.

Conclusions

Spectroscopic measurement of the burning toy fireworks including sparklers, torches and senko hanabi gave the following information. The emission intensity of burning sparklers and torches fluctuated owing to the non-homogeneous mixture of the firework compositions. In burning sparklers, color sparklers have characteristic visible spectral peaks, and spark sparklers have large K peaks and a small Na peak. The intense white-yellow light of spark sparklers comes from incandescent emissions of condensed phase sparks. The excitation purities of the sparklers were from 43% (blue) to 88% (iron). In burning torches, the emission intensities were in the following order:

falls > sparks > flame

The excitation purities of torches were from 2.9% (blue falls) to 87% (red flame). In burning senko hanabi, there are three burning steps: that is, the initial burning of senko hanabi composition, the fireball burning, and the developed fireball and branched sparks burning. The spectra of the fireball and the sparks were very similar suggesting that both emissions are incandescence from the condensed phase intermediate of the senko hanabi reaction.

References

1. W. Meyerriecks and K. L. Kosanke, "Color Values and Spectra of the Principal Emitters in Colored Flames", *Journal of Pyrotechnics*, Issue 18, Winter 2003, pp. 1–22.
2. T. Shimizu, "Manufacturing Process for Firework Compositions: Japanese Fireworks", in R. R. Lancaster, *Fireworks Principles and Practice*, Chemical Publishing Co., Inc., 4th edn, ch. 23, 2006, p. 394.

Burning Characteristics of Firework Stars and Lifting Charge

Morimasa Higaki, Dayu Ding, Yuzo Ooki, and Tadao Yoshida*
Ashikaga Institute of Technology
268-1 Ohmae-cho, Ashikaga-shi, Tochigi 326-8558, Japan
Tel: +81-284-62-0605, fax: +81-284-62-0976, email: yoshida@ashitech.ac.jp
*To whom all correspondence should be addressed.

Abstract: *Burning experiments were carried out for stars and lifting charge in the air and in a closed vessel. Three types of stars were used, that is, ordinary spherical, half-restricted spherical and hemispherical surface-restricted stars were used as models for flying burning. Partly restricted stars gave longer burning times than the ordinary stars, but not enough to explain the flying burning behavior. This was attributed to the burning of the ignition promoter in the restricted stars.*

The ratio of the time to maximum pressure to the stationary burning time of stars was about 0.44 and that of the lifting charge was about 0.24, presumably because the burning rate of the stars is smaller than that of the lifting charge.

Keywords: *firework stars, lifting charge, burning time, stationary burning, flying burning*

Introduction

The present authors have studied the ballistics of firework stars.[1,2] In the course of the study, it was shown that the flying burning time is longer than the stationary burning time of a star. Kosanke and Kosanke observed by means of a photograph that the burning star expelled from a shell in the air had a black part.[3] This may be the reason for the longer burning times of flying stars.

In order to determine the nature of flying burning, the burning times of ordinary and half-restricted stars are measured using an open cup by a high-speed video camera, and using a closed vessel by a pressure transducer. The burning time and pressure profile of the lifting charge are also measured using same methods as mentioned above and the results are discussed.

Experimental

Samples

The red peony and silver crown stars both for no. 5 shells (a Japanese no. 5 round shell corresponds to a western 6 inch shell) were supplied by Sunaga Hanabi Co. Ltd. in Ashikaga-city, and the lifting charge was made by Nippon Kayaku Co. Ltd. The restrictor was a mixture of an epoxy resin and a silicon polymer.

Three types of stars, as shown in Figure 1, were

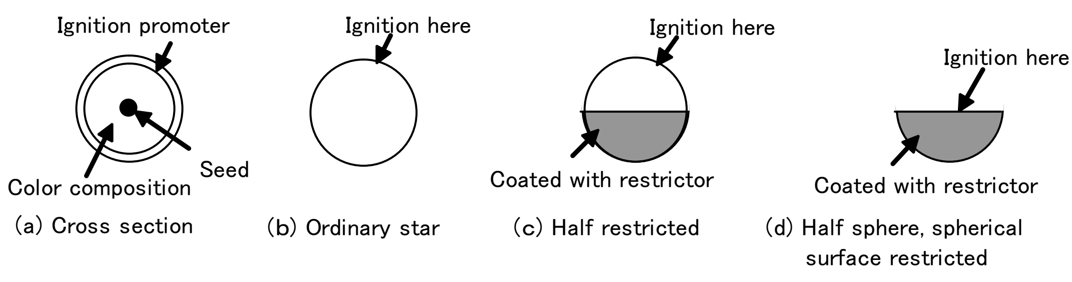

Figure 1. *Cross section and three types of stars used in the experiments.*

Table 1. *Results of the stationary burning times of stars in the open air.*

Sample	Shape	Run	Mass/g	Diameter/mm	Height/mm	Burning time/ms
Red peony star for no. 5 shell	Sphere	1		15.10		3416
		2	2.759	15.05		3252
		3	2.847	15.15		3515
		4	2.637	14.65		3265
		5	2.653	14.60		3294
		6	2.867	15.30		3190
		7	2.640	14.56		3305
		8	2.983	15.41		3366
		9	2.705	14.79		3229
	Mean		2.767	14.96		3315
	SD[a]		0.120	0.31		102
	RSD[b]		0.043	0.02		0.03
	Sphere (half-coated with restrictor)	10	2.850	15.10		4172
		11	2.716	14.95		4093
		12	2.862	15.00		4074
		13	2.714	14.90		4017
		14	2.827	14.85		4329
	Mean		2.794	14.96		4137
	SD[a]		0.073	0.10		121
	RSD[b]		0.026	0.01		0.03
	Half sphere (spherical surface coated with restrictor)	15	2.090	15.30	10.05	4417
		16	2.065	15.15	10.35	4205
		17	1.966	14.80	9.80	3983
		18	1.986	15.65	10.25	4084
		19	2.071	15.20	10.35	4233
	Mean		2.036	15.22	10.16	4184
	SD[a]		0.056	0.31	0.24	164
	RSD[b]		0.027	0.02	0.02	0.04

[a] Standard deviation. [b] Relative standard deviation (SD/mean).

used for stationary burning both in the open air and in a closed vessel. The stars were covered by an ignition promoter as shown in Figure 1 (a).

Stationary burning in the open air

Stationary burning in the open air was carried out in a draft chamber. A star was put on a heat resistant board in a stainless steel vat and ignited by a torch. The burning time was determined by a high-speed video camera (Phantom VRI-V4.2, 1000 frames s^{-1}).

The lifting charge was poured into a steel cup of 20 mm inner diameter and 20 mm depth placed on the heat resistant board. It was ignited by a Nichrome wire and the burning time was measured as mentioned above.

Table 1 (contd). *Results of the stationary burning times of stars in the open air.*

Sample	Shape	Run	Mass/g	Diameter/mm	Height/mm	Burning time/ms
Silver crown star for no. 5 shell	Sphere	20	3.462	15.05		4050
		21	3.320	14.75		3925
		22	3.315	14.70		3907
		23	3.239	14.75		4493
		24	3.594	15.10		4336
		25	3.250	14.61		3588
		26	3.315	14.85		4464
		27	3.331	14.95		3666
		28	3.075	14.53		4478
	Mean		3.322	14.81		4101
	SD[a]		0.144	0.19		355
	RSD[b]		0.043	0.01		0.09
	Sphere (half-coated with restrictor)	29	3.595	15.35		4238
		30	3.370	14.95		4237
		31	3.185	14.85		4126
		32	3.368	14.90		4157
		33	3.502	14.95		4195
	Mean		3.404	15.00		4191
	SD[a]		0.155	0.20		49
	RSD[b]		0.046	0.01		0.01
	Half sphere (spherical surface coated with restrictor)	34	2.025	14.90	8.95	4257
		35	2.030	14.95	8.67	4729
		36	2.266	15.25	9.40	4479
		37	2.355	15.10	9.70	4479
		38	2.055	14.85	9.15	3887
	Mean		2.146	15.01	9.17	4366
	SD[a]		0.154	0.16	0.40	316
	RSD[b]		0.072	0.01	0.04	0.07

[a] Standard deviation. [b] Relative standard deviation (SD/mean).

Stationary burning in a closed vessel

The stationary burning test in a closed vessel was carried out in a strand burning tester with 0.0011 m^3 inner volume. The pressure profile was measured and recorded by a pressure transducer, a pre-amplifier and a analyzing data recorder.

A star or lifting charge in the cup was put on a support, and the Nichrome wire was placed in contact with the surface of the sample. The support with the sample was set in the tester, and an electric current was sent through the wire and the sample was ignited. In the case of the hemispherical star, a small amount of the lifting charge was used for promoting the ignition of the cut surface of the star. The color stars used here were covered by

Table 2. *Results of the stationary burning of stars for no. 5 shells in the closed vessel.*

Sample	Shape	Run	Mass/g	Diameter/ mm	Height[c]/ mm	P_{max1} (10^5 Pa)	P_{max2} (10^5 Pa)	t_{max1}/ms	t_{max2}/ms	Mean t_s/ms	t_{max1}/t_s	t_{max2}/t_s
Red peony star for no. 5 shell	Sphere	1	2.814	14.92		1.148	0.873	308	1320	3315	0.09	0.40
		2	2.798	15.21		1.049	0.930	422	1320		0.13	0.40
		3	2.697	15.09		0.997	0.848	352	1760		0.11	0.531
		4	2.810	15.20		1.056	1.007	370	1540		0.11	0.47
		5	2.870	15.06		1.114	0.799	440	1320		0.13	0.40
	Mean		2.798	15.09		1.073	0.891	378	1452		0.11	0.44
	SD[a]		0.063	0.12		0.059	0.080	53	197		0.02	0.06
	RSD[b]		0.022	0.01		0.055	0.090	0.14	0.14		0.14	0.14
	Sphere (half-coated with restrictor)	6	2.891	15.14		1.040	1.138	572	1540	4137	0.14	0.37
		7	2.913	15.00		0.789	1.229	572	1672		0.14	0.40
		8	2.640	14.67		0.644	1.127	528	1848		0.13	0.45
		9	3.016	15.43		0.804	1.311	440	1980		0.11	0.48
		10	2.570	14.17		0.511	1.301	440	1936		0.11	0.47
	Mean		2.806	14.88		0.758	1.221	510	1795		0.12	0.43
	SD[a]		0.191	0.48		0.198	0.087	67	185		0.02	0.05
	RSD[b]		0.068	0.03		0.261	0.071	0.13	0.10		0.13	0.10
	Half sphere (spherical surface coated with restrictor)	11	2.224	15.38	10.09	0.707	1.111	1144	1672		0.27	0.40
		12	2.580	16.17	11.35	0.636	1.060	1496	3080		0.36	0.74
		13	2.108	15.46	10.22		1.144		2288	4184	0.00	0.55
		14	2.075	15.19	10.15	0.634	1.000	1276	2992		0.31	0.72
		15	1.931	14.89	9.73	0.662	1.111	1364	2992		0.33	0.72
	Mean		2.184	15.42	10.31	0.660	1.085	1320	2605		0.32	0.62
	SD[a]		0.245	0.48	0.61	0.034	0.056	148	612		0.14	0.15
	RSD[b]		0.112	0.03	0.06	0.052	0.052	0.11	0.23		0.46	0.24

[a] Standard deviation. [b] Relative standard deviation (SD/mean). [c] Height of the half sphere.

an ignition promoter. The cut surface without the ignition promoter was difficult to ignite by means of the electrically heated wire only.

Results and Discussion

Stationary burning of stars in the open air

Results of the stationary burning in the open air and in the closed vessel are listed in Tables 1 and 2, respectively. Examples of the pressure profiles of the burning stars in the closed vessel are shown in Figure 2a/2b.

It is seen from Table 1 that the burning time of the silver crown star is longer than that of the red peony star with the same geometry. The burning times of the three types of a star increased in following order:

Spherical star without resin coating < spherical star with half surface coated by resin < hemispherical star with spherical surface coated by resin

Some burning characteristics of these stars are shown from Figure 2. For spherical stars without resin coating, an initial steeper pressure rise was observed. Then the pressure dropped once, then

Table 2 (contd). *Results of the stationary burning of stars for no. 5 shells in the closed vessel.*

Sample	Shape	Run	Mass/g	Diameter/ mm	Height[c]/ mm	P_{max1} (10^5 Pa)	P_{max2} (10^5 Pa)	t_{max1}/ms	t_{max2}/ms	Mean t_s/ms	t_{max1}/t_s	t_{max2}/t_s
Silver crown star for no. 5 shell	Sphere	1	3.392	14.84		1.067	1.406	440	1760	4101	0.11	0.43
		2	3.447	15.03		1.020	1.360	528	1980		0.13	0.48
		3	3.250	14.77		0.954	1.288	484	1892		0.12	0.46
		4	3.283	14.48		1.055	1.439	440	1892		0.11	0.46
		5	3.280	15.03		1.173	1.454	475	1848		0.12	0.45
	Mean		3.330	14.83		1.054	1.389	473	1874		0.12	0.46
	SD[a]		0.085	0.23		0.080	0.067	36	80		0.01	0.02
	RSD[b]		0.025	0.02		0.076	0.048	0.08	0.04		0.08	0.04
	Sphere (half-coated with restrictor)	6	3.340	14.71		0.485	1.494	352	2552	4191	0.08	0.61
		7	3.368	15.50		0.608	1.583	372	2552		0.09	0.61
		8	3.450	15.00		0.713	1.429	440	2376		0.11	0.57
		9	3.274	14.70		0.423	1.252	370	2728		0.09	0.65
		10	3.410	15.16		0.561	1.449	528	2596		0.13	0.62
	Mean		3.368	15.01		0.558	1.441	412	2561		0. 10	0.61
	SD[a]		0.067	0.34		0.112	0.121	73	126		0.02	0.03
	RSD[b]		0.020	0.02		0.201	0.084	0.18	0.05		0.18	0.05
	Half sphere (spherical surface coated with restrictor)	11	2.463	14.88	10.08	0.627	1.350	1144	3608	4366	0.26	0.83
		12	2.066	14.74	9.14		1.514		3960		0.00	0.91
		13	2.392	15.16	9.78	0.570	1.302	1428	3256		0.33	0.75
		14	2.260	14.84	9.43	0.544	1.236	1760	4268		0.40	0.98
		15	2.298	14.73	9.49	0.631	1.213	1188	3080		0.27	0.71
	Mean		2.296	14.87	9.58	0.593	1.323	1380	3634		0.316	0.83
	SD[a]		0.151	0.17	0.36	0.043	0.120	282	490		0.152	0.11
	RSD[b]		0.066	0.01	0.04	0.072	0.090	0.20	0.13		0.481	0.14

[a] Standard deviation. [b] Relative standard deviation (SD/mean). [c] Height of the half sphere.

high pressure continued and the pressure decreased to a constant value corresponding to the end of burn.

The initial steeper pressure rise may be due to the rapid burning of the ignition promoter coating the less ignitable color composition of the star. The next pressure rise is due to the burning of the main color composition of the star.

The maximum pressures P_{max1} of the first peak of the profiles of the silver crown and red peony stars were similar. The second peak pressures $P_{max2}$of both stars were different, that is, the second peak pressure of the silver crown star was higher than that of the red peony star suggesting that the combustion temperature and/or gas production of the former is higher than that of the latter.

The burning times of the stars were not estimated from the pressure profiles of the burning test in the closed vessel. The burning times of stars can be determined by a high-speed video camera record of the duration of the combustion flame in the stationary burning test in the open air. The mean ratios of the time to maximum pressure to

Table 3. *Mean ratios of various burning times to the stationary burning times of stars.*

Star	Condition	Mean ratio	Reference
Blue peony, silver peony and silver crown	Flying	$t_f/t_s = 1.6$	1
Silver crown for no. 4 shell	Flying	$t_f/t_s = 1.4$	2
Silver crown for no. 5 shell	Flying	$t_f/t_s = 1.5$	2
Red peony for no. 5 shell	Coated by resin[a]	$t_{sc1}/t_s = 1.25$	This work
Red peony for no. 5 shell	Coated by resin[b]	$t_{sc2}/t_s = 1.26$	This work
Silver crown for no. 5 shell	Coated by resin[a]	$t_{sc1}/t_s = 1.02$	This work
Silver crown for no. 5 shell	Coated by resin[b]	$t_{sc2}/t_s = 1.06$	This work

[a] Half the sphere is coated by the resin. [b] Hemisphere with spherical surface coated by the resin.

the flame duration time were similar (about 0.45) for both spherical silver crown and red peony stars without resin coating. The reason for the difference in burning times between the closed vessel and the open air may be attributable to a property of the pressure profile of burning spherical stars and the pressure effect on the burning rate of stars.

For the half-resin-coated spherical star, the maximum pressure of the first peak was smaller than that of the star without resin coating, presumably because the exposed amount of the ignition promoter of the former was half that of the latter. The time to maximum pressure of the second peak of the half-coated star was longer than that of the star without resin coating.

For the hemispherical star with the spherical surface coated, the shape of the profiles was different from other types of stars. There were two step pressure increases, of which the first was a little steeper and the second was a little gentler. The first steeper pressure rise seems to be due to the burning of the ignition promoter coated by the restrictor. The burning of the sandwiched promoter may be slower than that of the exposed promoter and faster than that of the color composition of the star.

The time to the maximum pressure of a star increased in the following order:

Spherical star without resin coating < spherical star with half surface resin coating < hemispherical star with spherical surface resin coated

Comparison of the times of flying and stationary burning

Table 3 lists the mean ratios of the times of the flying and stationary burning of stars.

Table 4. *Stationary burning time of the lifting charge in the cup.*

Run	LC/g	Burning time/ms	Run	LC/g	Burning time/ms
1	1.0	114.2	6	2.0	149.0
2	1.0	140.0	7	2.0	124.4
3	1.0	114.6	8	2.0	120.2
4	1.0	111.4	9	2.0	109.6
5	1.0	112.6	10	2.0	142.8
Mean		118.6	Mean		129.2
SD[a]		12.1	SD[a]		16.3
RSD[b]		0.102	RSD[b]		0.126

[a] Standard deviation. [b] Relative standard deviation (SD/mean).

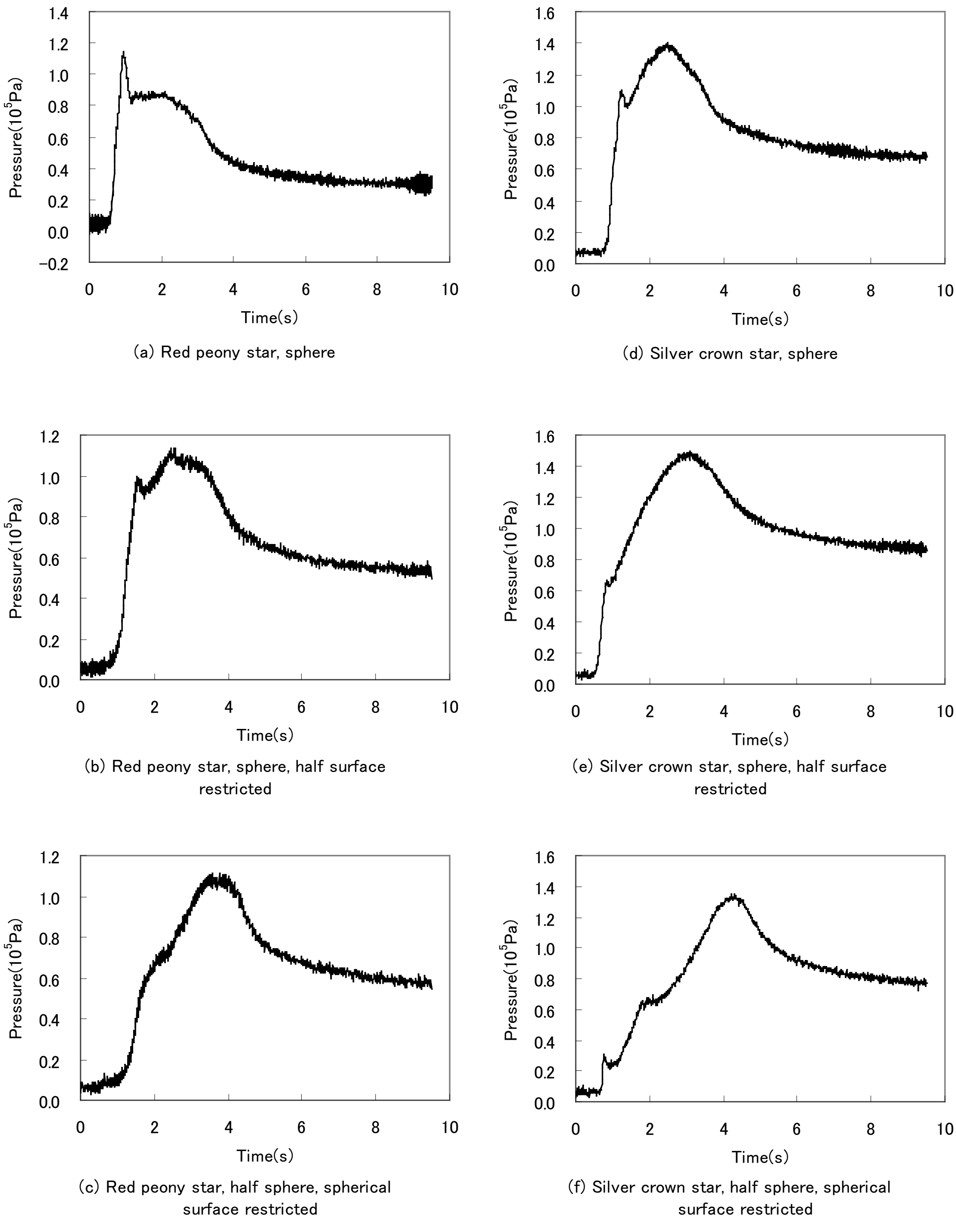

Figure 2. *Examples of the pressure profiles of burning stars in the closed vessel.*

The partial restriction of the surface of stars resulted in longer burning times, but not enough to explain the longer flying burning times. This may be due to the burning of ignition promoter remaining between the color composition and the restrictor.

Burning characteristics of the lifting charge

The stationary burning times of the lifting charge are listed in Table 4 and examples of the pressure

Table 5. *Summary of the burning experiments of the lifting charge in the open cup and in the closed vessel.*

Run	LC/g	P_{max} (10^5 Pa)	t_{max}/ms	Mean t_s/ms	t_{max}/ts
1	1.0	3.397	24.2		0.20
2	1.0	2.979	28.6		0.24
3	1.0	2.959	30.8	118.6	0.26
4	1.0	2.230	28.6		0.24
5	1.0	2.808	30.8		0.26
Mean		2.874	28.6		0.24
SD[a]		0.422	2.7		0.02
RSD[b]		0.147	0.1		0.09
6	2.0	5.251	30.8		0.24
7	2.0	5.453	30.8		0.24
8	2.0	5.548	30.8	129.2	0.24
9	2.0	5.381	28.6		0.22
10	2.0	5.600	30.8		0.24
Mean		5.447	30.4		0.23
SD[a]		0.138	1.0		0.01
RSD[b]		0.025	0.0		0.03

[a] Standard deviation. [b] Relative standard deviation (SD/mean).

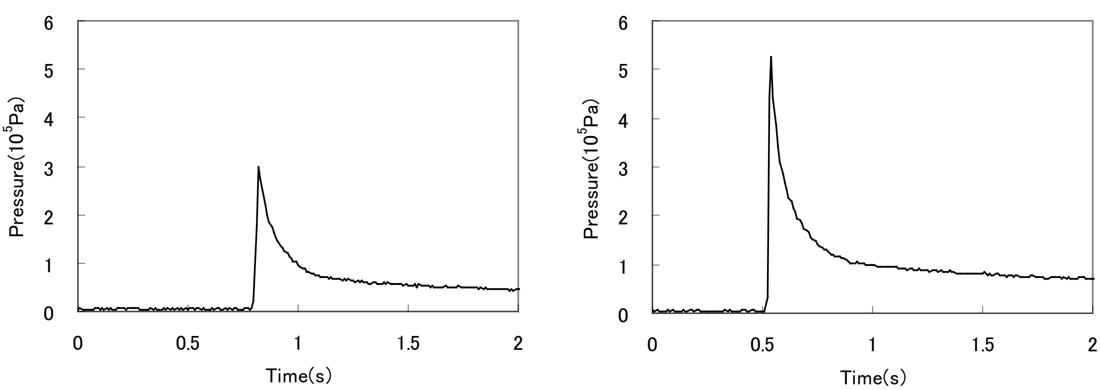

(a) LC 1.0g

(b) LC 2.0g

Figure 3. *Examples of the pressure profile of burning lifting charge in the closed vessel.*

profiles of the lifting charge in the closed vessel are shown in Figure 3.

The mean ratio of the time to maximum pressure to the stationary burning time (t_{max}/t_s) was 0.26 which is smaller than that of about 0.45 for burning of the ordinary stars, presumably because of the higher burning rate of the lifting charge than that of the stars.

A burning experiment using lifting charge was done in a closed vessel and in the open air by Shibata, Hasegawa *et al.*[4]). A sample of the lifting charge was poured into a plastic tube of 7 mm inner diameter and 30 mm depth. The times to maximum pressure in the closed vessel and the burning time in the open air were 100 ms and 270 ms, respectively. The ratio of the time to the maximum pressure to the burning time in the open air (t_{max}/t_s) was 0.37.

Acknowledgement

The authors wish to gratefully acknowledge the assistance of Sunaga Hanabi Co. Ltd. and Nippon Koki Co. Ltd. for the experiments.

References

1 Y. Ooki, D. Ding, M. Higaki and T. Yoshida, "Burning and Air Resistance of Fireworks Stars", *Science and Technology of Energetic Materials*, in contribution.

2 Y. Ooki, D. Ding, M. Higaki and T. Yoshida, "Exterior Ballistics of Firework Stars (1) Trajectories of Stars with Long Burning Time", *Journal of Pyrotechnics*, in press (this issue).

3 K. L. Kosanke and B. J. Kosanke, "Stars Blown Blind", Selected Pyrotechnic Publications of K. L. and B. J. Kosanke, Part 4, page 1 (1999), originally appeared in *American Fireworks News*, No.160, 1995.

4 H. Shibata, "A Study on the Burning Velocity Evaluation by a Strand Tester", Master Dissertation, Yoshida Laboratory, Hosei University, 1997; T. Hasegawa, H. Shibata, T. Nojima, K. Hara and T. Yoshida, "The Evaluation of the Burning Characteristics of Energetic Materials by a Strand Tester", *Studies of Disasters*, Vol. 27, 1996, p. 201.

Exterior Ballistics of Firework Stars

Yuzo Ooki, Dayu Ding, Morimasa Higaki, and Tadao Yoshida*
Department of Mechanical Engineering, Ashikaga Institute of Technology,
268-1 Ohmae-cho, Ashikaga-shi, Tochigi 326-8558, Japan
Tel: +81-284-62-0605, fax: +81-284-62-0976, email: yoshida@ashitech.ac.jp
* To whom all correspondence should be addressed.

Abstract: *Burning and shot experiments have been carried out to examine the burning time and the trajectory of burning firework stars. The burning time in flight was longer than the stationary burning time. The trajectory of a burning star in the air was modeled assuming the linear burning rate of the star and* $C_D = at + b$. *It was found that there are sometimes abnormal trajectories and interruption of the burning during flight for a large star with high initial velocity.*

Keywords: *Exterior ballistics, firework star, burning rate, initial velocity*

Introduction

Firework stars with long burning times are used in willow and crown aerial fireworks. The exterior ballistics of burning stars of this type is important for the design of the shape of the willow and crown.

Shimizu has studied the ballistics of burning stars expelled from exploded shells.[1,2] Kosanke and Kosanke reported the partial burning of the expelled stars.[3] Kosanke and Kosanke[4] and Mercer[5] have modeled the exterior ballistics of aerial firework shells.

In the present work, measurement of the burning time of stationary and flying stars was carried out, and the trajectory of the fired stars was observed. Then, the observed data were analyzed.

Experimental

Samples

The silver crown stars for no. 2.5, 4 and 5 shells (a Japanese no. 2.5 round shell corresponds to a western 3 inch shell) were supplied by Sunaga Fireworks Company at Ashikaga-city, and the lifting charge and electric match were made by Nippon Kayaku Company.

The mortars

The two mortars used for firing stars were made of steel, with inner diameters of 15 mm and 20 mm, and depths of 270 mm and 360 mm, respectively.

Experimental method

A star was placed on a heat resistant board and ignited with a torch. The stationary burning time of the star was determined using a high-speed video camera (Phantom VR-V4.2) with a frame rate of 1000 frames s^{-1}. An electric match was placed on the bottom of the mortar, and the lifting charge was poured into the vertical mortar from the muzzle. The electric match was ignited by an electric current from a 12 V battery and then the lifting charge was ignited immediately by the match. The trigger of the high-speed video camera worked simultaneously with the turning on of the electric current.

The trajectory and burning time of the star were observed and recorded by the high-speed video camera with a frame rate of 1000 frames s^{-1} at a point 100 m away from the mortar.

Analysis of the motion of a star in the air

The motion of a burning star fired vertically in the air is expressed by following equation (1):

$$\frac{\mathrm{d}u}{\mathrm{d}t} = -g - \frac{3\rho_{\mathrm{air}}}{4\rho_{\mathrm{star}}} \times \frac{C_{\mathrm{D}}}{D_{\mathrm{star}}} \times |u| \times u \qquad (1)$$

or

$$\frac{\mathrm{d}u}{\mathrm{d}t} = -g - k \times |u| \times u \qquad (2)$$

Here u, t, g, ρ_{air}, ρ_{star}, D_{star} and C_{D} are the velocity of the star, flying time, acceleration under gravity, air density, density of the star, diameter of the star and drag coefficient of air, respectively. The velocity u is positive when the star moves upward.

and

$$k = \frac{3\rho_{air}}{4\rho_{star}} \times \frac{C_D}{D_{star}} = \frac{3\rho_{air}}{4\rho_{star}} \times K \qquad (3)$$

It was assumed that the mass and cross section of a star change but the density of the star does not change with time. Therefore, the second term on the right side of equation (1) for the air drag is proportional to the air drag coefficient C_D and inversely proportional to the diameter of the star. Finally, this term is proportional to K (= C_D/D_{star}).

The value of K was obtained by fitting the calculated trajectory to the observed one of the fired star. The diameter D_{star} of the star is a function of the flying time of the star and is calculated from the mean linear burning rate of stars. Then, C_D was calculated from K and D_{star} using equation (3).

Results and discussion

Stationary and flying burning times of stars

The stationary and flying burning times of stars are listed in Table 1.

The flying burning time was longer than the stationary burning time.[6] In the present work, this nature was confirmed. The ratio of the flying burning time to the stationary burning time (t_f/t_s) was 1.44–1.67 for stars of no. 2–6 shells in the previous work,[6] and 1.36 and 1.46 in the present work for the stars of no. 4 and no. 5 shells, respectively.

One of reasons that the flying burning time is longer than the stationary burning time may be partial burning in the flight of a star. Kosanke and Kosanke showed by means of a photograph that part of the star expelled from an exploded shell was black, indicating that part of the flying star was flameless. The flame at the front surface of the expelled star might be extinguished by the high-speed air-flow and result in a slower burning rate of the star. Another possible reason might be the cooling effect of air-flow around the burning star.

Fit of *K*

The value of K obtained by fitting the calculated trajectory to the observed one gave good agreement between the observed and calculated trajectories of vertically fired stars for 25 cases among 32 shots. However, no good agreement was obtained for 7 cases and no data for one case. Examples of good agreement and poor agreement are shown in Figure 1.

At the moment, the cases where poor agreement was obtained were the cases where the initial velocities were low and the burning stars dropped on the ground.

In the present work, most of the stars for a no. 5 shell with a 2 g lifting charge (LC) failed to continue burning until complete combustion. The interruption of burning may be attributed to the high-speed air-flow around the burning star. In the other case, the flame at the star disappeared once and then the flame appeared again in the course of flying.

Figure 2 shows some examples of the plot of calculated C_D against time for the cases where there was good agreement.

Table 1. *Stationary and flying burning time of the silver crown stars.*

		Mass/g		Diameter/mm		Burning time/s		t_f/t_s
		Mean	RSD	Mean	RSD	Mean	RSD	
Stars for no. 2.5 shell	Stationary	2.734	0.024	13.908	0.021	3.601	0.073	
	Flying	2.747	0.048	13.862	0.019			
Stars for no. 4 shell	Stationary	4.737	0.037	16.565	0.013	4.198	0.042	1.36
	Flying	4.964	0.027	16.840	0.014	5.701	0.047	
Stars for no. 5 shell	Stationary	5.592	0.029	17.636	0.014	4.646	0.043	1.46
	Flying	5.640	0.028	17.624	0.012	6.761	0.030	

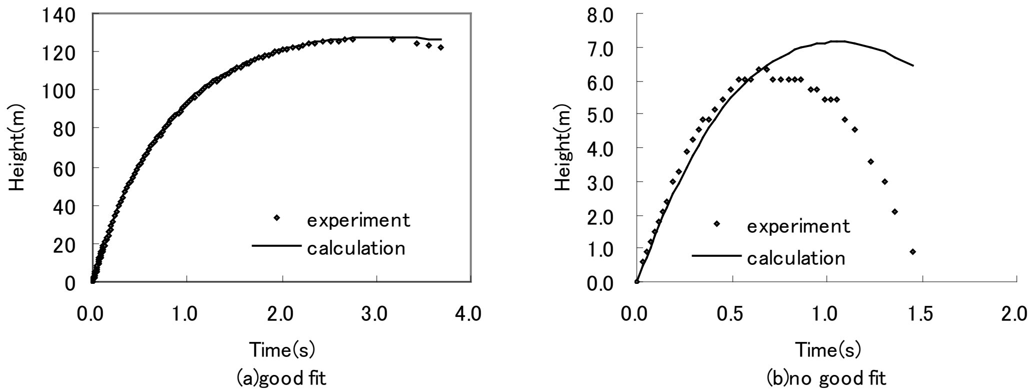

Figure 1. *Examples of plot of flying height vs. flying time of star.*

All calculated trajectories using these C_D values agreed well with the observed trajectories, but the C_D values were scattered at later times. Also two abnormal C_D values were obtained (runs 11 and 21).

Modeling of the motion of the fired star

The trajectory of a fired star in the air was modeled by following procedures:

(1) K in equation (3) is obtained as a function of time by fitting the calculated trajectory to the observed trajectory of a fired star and both trajectories are plotted in the time–height coordinates (Figure 3(a)).

(2) C_D is obtained as the function of time from K and D_{star} using equations (3) and (4) (Figure 3(b)).

$$D_{star} = D_{star0} - 2r_{star}t \qquad (4)$$

(3) C_D has little effect on the air drag when the velocity is small as shown in ref. 7. As shown in Figure 3(c), the flying velocity of the star becomes small after 2 seconds after the shot in this case.

(4) C_D is assumed to be a linear function of flying time before the star arrives at its maximum height (Figure 3(d)). In this case the following equation was obtained for approximate C_{Da}:

$$C_{Da} = 0.4589t + 0.2864 \qquad (5)$$

(5) An approximate value for K_a is calculated using equations (3), (4) and (5) (Figure 3(e)).

(6) The approximate trajectory of the burning star is estimated using K_a and the agreement between the calculated and observed trajectories is confirmed (Figure 3(f)).

Table 2 lists the conditions of the experiment and

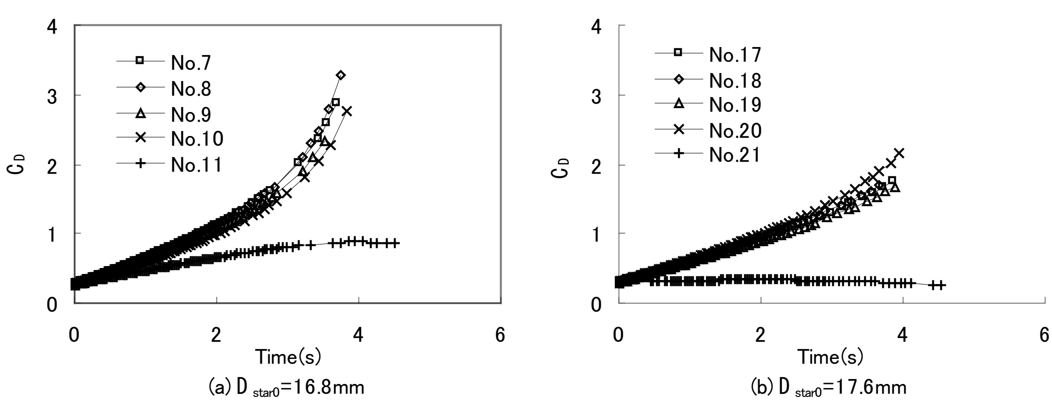

Figure 2. *Plot of calculated C_D vs. time. LC = 1.0 g.*

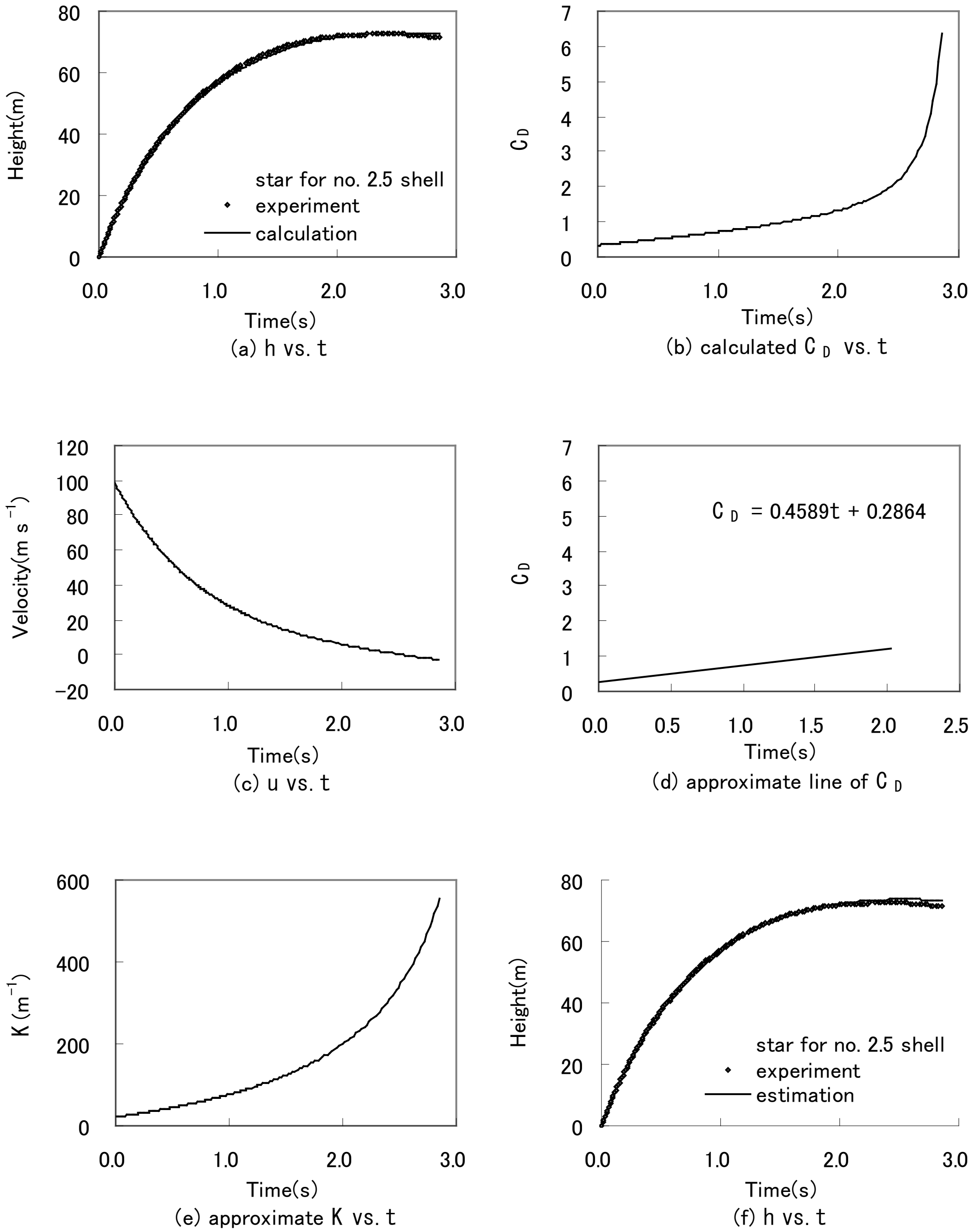

Figure 3. *Modeling of the motion of a star in the air.*

the results.

The mean values of initial diameter $\bar{D}_{\text{star}0}$, linear burning rate $\bar{r}_{\text{star}}$, and lifting charge (LC) of stars for runs 7, 8, 9, 10 and runs 17, 18, 19, 20 are listed in Table 3, respectively.

The calculated maximum height attained and the time to the maximum height of the stars using these mean parameters are listed in Table 3. The results can be compared to the observed values listed in Table 2. The calculated mean trajectory and observed trajectories are shown in Figure 4. The calculated drag coefficient C_D increased with time and the initial values were about 0.26 though there were some exceptions. At the moment, the reason for these phenomena is not clear.

Table 2. *Experimental conditions and results.*

No.	D_{star0}/mm	LC/g	u_0/m s^{-1}	Mortar diam. /mm	Fit to K	$C_D = at+b$		h_{max}/m		t_{max}/s	
						a	b	Obs.	Calc.	Obs.	Calc.
1	13.4	1.00	98	15	yes	0.4589	0.2864	72.5	73.7	2.490	2.529
2	13.8	1.00	15	15	no						
3	14.2	1.00	31	15	no						
4	14.0	1.00	218	15	yes	0.0574	0.3032	162.7	160.7	3.792	3.702
5	14.0	1.00	36	15	no						
6	13.8	2.00		15	no data						
7	16.8	1.00	168	20	yes	0.4267	0.2546	126.3	126.8	2.760	2.964
8	16.4	1.00	168	20	yes	0.4143	0.2599	125.7	127.4	2.807	3.002
9	16.8	1.00	156	20	yes	0.3782	0.2619	121.5	123.3	2.782	3.024
10	17.0	1.00	144	20	yes	0.36	0.2592	121.5	118.0	2.975	3.109
11	16.9	1.00	168	20	yes	0.1909	0.2688	145.9	145.3	3.313	3.469
12	17.3	2.00	217	20	yes	0.2805	0.2374	163.6	165.1	3.185	3.390
13	17.0	2.00	217	20	yes	0.1896	0.3047	159.1	158.5	3.393	3.505
14	16.7	2.00	241	20	yes	0.1044	0.3066	*170.8*[a]	185.1	*2.357*	3.782
15	16.8	2.00	205	20	yes	0.1069	0.3494	155.2	155.5	3.410	3.571
16	16.7	2.00	265	20	no						
17	17.3	1.00	165	20	yes	0.3442	0.2699	130.8	131.6	2.972	3.208
18	17.3	1.00	158	20	yes	0.3485	0.2845	126.9	127.6	3.124	3.190
19	17.6	1.00	165	20	yes	0.321	0.2823	135.6	134.4	3.228	3.278
20	17.6	1.00	180	20	yes	0.396	0.2632	135.9	137.6	3.176	3.254
21	17.9	1.00	165	20	yes	0.0208	0.3017	*171.4*[a]	172.2	*4.104*	4.266
22	17.5	2.00	256	20	yes	0	0.15	*22.3*[b]	365.6	*0.092*	5.980
23	18.0	2.00	263	20	yes	0	0.15	*21.7*[b]	364.9	*0.088*	6.016
24	17.6	2.00	218	20	yes	0	0.15	*20.5*[b]	332.8	*0.100*	5.900
25	17.6	2.00	256	20	yes	0.0822	0.3242	170.2	192.9	1.956	3.876
26	17.6	2.00	271	20	yes	0	0.15	*20.2*[b]	365.7	*0.080*	5.840
27	17.9	0.25	60	20	no						
28	17.3	0.50	90	20	no						
29	17.8	0.75	135	20	yes	0.4597	0.2359	115.2	113.5	2.896	3.024
30	17.6	1.25	180	20	yes	0.244	0.2836	149.5	148.9	3.540	3.378
31	17.8	1.50	226	20	yes	0.0097	0.3193	*171.1*[a]	201.9	*2.112*	4.312
32	17.5	1.75	248	20	yes	0.0125	0.3788	*170.8*[a]	189.0	*2.488*	4.056

Note: The data in italics are not really the maximum height and the time to maximum height of a star because (a) it went out of sight of the camera before it arrived at its maximum height or (b) its burn was interrupted and the rest of the trajectory could not be recorded by the camera.

Abnormal and interrupted burning trajectories

Sometimes abnormal trajectories of the burning stars were observed. For example, the trajectories of runs 11 and 21 were different from other groups of the same initial conditions. In the equation

$$C_D = at + b,$$

the values of a are different from other groups, though the values of b are similar to those of other groups. In reality, abnormal flights occur sometimes.

The other characteristics of the abnormal

Table 3. *Experimental conditions, mean calculated parameters, and calculated and observed trajectories of the burning stars.*

No.	D_{star0} /mm	r/mm s^{-1}	u_0/m s^{-1}	LC/g	$C_D = at + b$		h_{max}/m	t_{max}/s
					a	b	Calc.	Calc.
Runs 7–10	16.8	1.49	159	1.0	0.395	0.259	129.1	3.163
Runs 17–20	17.5	1.32	167	2.0	0.352	0.275	137.4	3.167

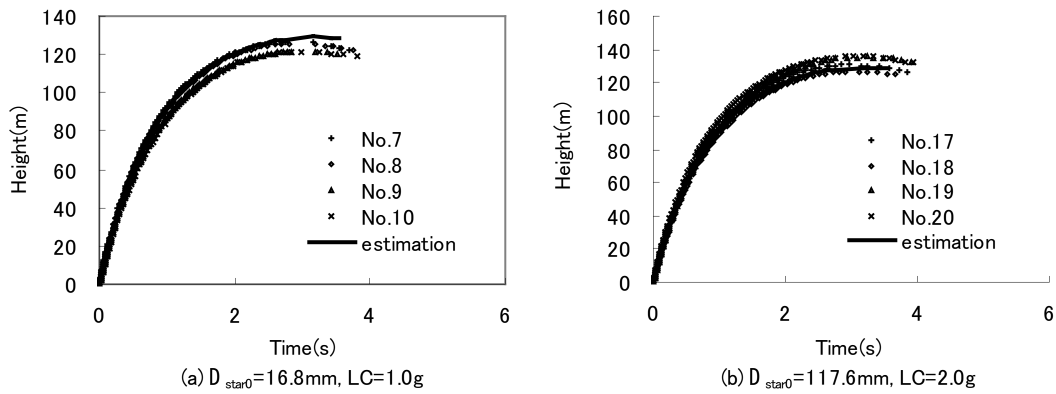

Figure 4. *Calculated mean trajectory and observed trajectories of burning stars with (a) D_{star0} = 16.8 mm and LC = 1.0 g, (b) D_{star0} =17.6 mm and LC = 2.0 g.*

trajectories are higher maximum height attained and longer time required to attain maximum height. These phenomena may be attributable to the slower burning speeds of stars with abnormal trajectories than those of normal ones.

Also, interruption of burning took place with large stars (for no. 5 shells) and large lifting charges (2.0 g). It is known that the flames of stars expelled from a burst shell are sometimes partly extinguished.[3] In our case, the flames of the stars were blown out completely.

In the case of the blown-out flames, the values of a and b in the C_D equation are both smaller than those in normal flight. The shape of the flame of the burning stars in the interrupted case might be different from that of normal burning stars.

Effect of the amount of lifting charge on the trajectories

The amount of lifting charge affects the parameters a and b. The value of a decreases and that of b increases with increasing amount of lifting charge. With the stars of no. 5 shells, burning of the stars was interrupted with 2.0 g LC in which the a values were much smaller than those of normal cases.

Conclusions

(1) The burning time of a star in flight is longer than the stationary burning time, presumably because of the cooling effect of the flowing air around the star.

(2) The trajectory of a burning star in the air was modeled assuming a linear burning rate of the star and $C_D = at + b$. This method is not valid for the falling trajectory.

(3) It was found that there are sometimes abnormal trajectories and interruption of burning during flight for high initial velocity and large stars.

Acknowledgement

The authors wish to gratefully acknowledge the assistance of Sunaga Hanabi Company, Showarika Company, and the undergraduate students of the Higaki Laboratory: Arima, Ariga, Kashiwa and Hukazawa.

References

1 T. Shimizu, "Conditions for Designing Japanese Fire-Display-Shells of Chrythanthemum Type (1)", *Journal of the Industrial Explosives Society, Japan*, 17(4), 1956, p. 251.

2 T. Shimizu, "Conditions for Designing Japanese Fire-Display-Shells of Chrythanthemum Type (2)", *Journal of the Industrial Explosives Society, Japan*, 18(1), 1957, p. 50.

3 K. L. Kosanke and B. J. Kosanke, "Stars Blown Blind", Selected Pyrotechnic Publications of K. L. and B. J. Kosanke, Part 4, p. 1 (1999), Originally appeared in *American Fireworks News*, No. 160, 1995.

4 K. L. Kosanke and B. J. Kosanke, "Computer Modeling of Aerial Shell Ballistics", *Pyrotechnica*, XIV, 1992, p. 80.

5 J. E. Mercer, "Thermodynamics of Black Powder and Aerodynamics of Propelled Aerial Shells", *Journal of Pyrotechnics*, Issue 16, Winter 2002, p. 37.

6 Y. Ooki, D. Ding, M. Higaki and T. Yoshida, "Burning and Air Resistance of Fireworks Stars", *Science and Technology of Energetic Materials*, Vol. 67, No. 1, 2006, p. 39.

7 Y. Ooki, D. Ding, M. Higaki and T. Yoshida, "Air Resistance of Spherical Fireworks Shells", *Science and Technology of Energetic Materials*, Vol. 67, No. 1, 2006, p. 43.

Evaluation Of Multi-shot Firework Articles Using Mortar Recoil Measurements

R. Guilbeault and E. Contestabile
CANMET Complex – Building 12, 555 Booth Street, Ottawa, ON K1A 0G1, Canada

Abstract: *Recoil from fireworks articles often arises as a concern in accident investigations or when fireworks are launched from unconventional locations such as rooftops, or other light building elements such as overhangs, from decks of small bridges or those of barges. In this latter case, the Authority Having Jurisdiction will typically require some assurance that the structure will not be damaged and is sufficiently robust to support the dynamic loads resulting from the function of the firework articles. In this study, it is proposed that such measurements can also be used to evaluate multi-shot devices since; their recoil load history reflects their performance in time and magnitude.*

Various researchers have, over the last decade, devised means to measured recoil loads. Piezoelectric load cells, which have fast response time, have been used and found to satisfactorily track the fireworks recoil loads. This study presents data obtained using an apparatus in the form of a 25-cm diameter platform. Fireworks mortars or articles are placed and functioned on the platform. The signal from the piezoelectric load cell is recorded by a digital storage oscilloscope.

The results indicate that the recoil history can be used to determine inter-shot times, total duration, and relative launch heights of the effects of the multi-shot article. In addition, defective launches and other modes of failure such as in timing can also be easily identified.

Keywords: *multi-shot fireworks, recoil, load cell, RLP, mortar*

Introduction

The Canadian Explosives Research Laboratory (CERL), as part of its mandate, evaluates firework articles intended for sale and use in Canada. Part of the evaluation process is testing the articles' performance. Articles must meet certain minimum performance requirements which are given by the standards outlined in the Family and Display Fireworks Criteria[1] document. Standard test procedures at CERL require articles to be functioned and the performance, in terms of hazards or malfunctions, evaluated. This evaluation is based on visual observations and video records.

The evaluation of multi-shot articles such as Bombardo boards and cakes can become difficult primarily because of the often high number of shots constituting the article. Also, many products have several different effects incorporated into the mix. To facilitate a more comprehensive evaluation of the performance of such articles a load cell device was used to monitor the recoil forces generated when an effect is projected from the article. Such a record can provide quality indicators such as consistency of timing, projection heights and overall function time.

A number of tests were performed on professional class cakes and their recoil assessed with the load cell device. The performance and the recoil force records obtained are presented and discussed. Recommendations as to the usefulness of such a tool for the evaluation of multi-shot firework devices are also made.

Experimental Set-up

A load cell device, henceforth referred to as the Recoil Load Platform (RLP), was constructed specifically for measuring recoil forces generated by firework mortars. The construction is shown in Figure 1. This device was initially used for the evaluation of the recoil loads from large diameter fireworks.[2,3]

The RLP clamps and pre-stresses a piezoelectric force ring transducer so that it can track recoil loads and the associated rebound. The force ring is connected to a signal conditioner which in turn is connected to a digital oscilloscope with a 16-bit input module that provides the gain and high resolution required for the low range of recoil forces produced by these fireworks articles. The calibrated range of the force ring used was 0 to 60 000 lbf. Data were collected at a sampling rate of 5 kHz over a 90 s period.

The fireworks sample was placed on the RLP and functioned without any additional stabilization or support (Figure 2).

Results and Discussion

A total of 15 tests were conducted on six types of articles with the number of shots ranging from 19 to 49. A description of the articles tested is given in Table 1, with two of the samples being shown on the RLP in Figure 2. Note that some of the articles described in Table 1 do not have masses indicated because they were not declared by the manufacturer.

All articles tested were of similar size and had similar tube diameters, however the amount of lift charge per tube varied substantially. These articles varied in base sizes and some overhung the surface area of the RLP. As a result, some of the tubes were not supported directly on the base.

Also, the firing sequence varied according to the design. The mixed effect cakes fired different effects in groups of 7 for a total of 49 shots. This made interpretation of the recoil data more difficult. A video record was needed to correlate the effect-type to the projection height and the recoil force. A typical recoil record is shown in Figure 3.

The profile displays a distinct record of the recoil force for each shot for this article. The total number of shots, the interval between shots and the total function time can easily be extracted from the record. A detailed view of the load profile of a

Figure 2 *Cakes on recoil base.*

single shot is shown in Figure 4. Each shot often exhibited a similar pattern with a double peak and subsequent lower magnitude perturbations. These signals can be attributed to materials being projected, decoupling of the multi-shot article from the recoil base and from the response characteristics of the RLP. As seen in Figure 5 these patterns have similar trends.

The magnitude of the recoil force, the intervals between firings and the duration of each of the 15 articles tested were extracted from the records and

Table 1 *Firework specifications.*

Article identification	Effect	Number of shots	Tube diameter/ mm	Declared mass/g			Duration/s
				Gross	NEQ	Lift/tube	
A	Reports	49	32	N/A	N/A	N/A	N/A
B	Star shell	19	24	1600	180	2.0	N/A
C	Mixed	50	24	N/A	N/A	N/A	N/A
D	Mixed	49	32	7620	1190	5.0	40
E	Mixed	49	32	6180	1100	4.7	N/A
F	Mixed	49	39	11300	1715	9.2	40

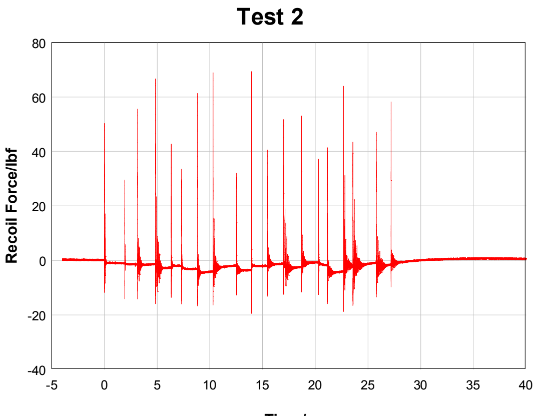

Figure 3 *Typical recoil profile of Article B.*

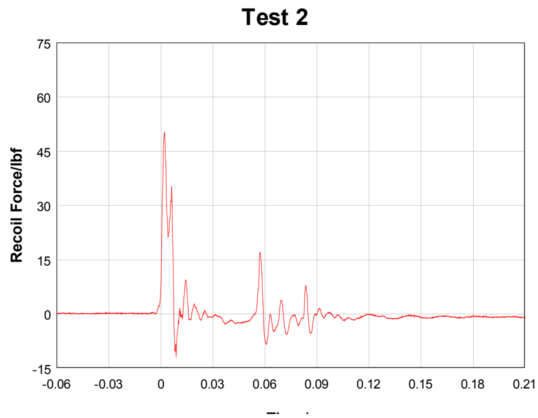

Figure 4 *Expanded view (Shot #1).*

summarized in Table 2.

Recoil forces vary from tube to tube, and they and the corresponding impulses have not been correlated to the projection heights of the pyrotechnic effects. Even groupings of similar effects displayed a wide variation in recoil forces (Figure 6).

The quality of the tube and fit of the components or shells influence the recoil forces recorded. If a shell or component fits very tightly, then there will be a greater pressure built up within the tube. This results in the pyrotechnic effect being ejected with a greater force and this is reflected in a higher recoil force. If the fit is very loose then the tube pressure will be lower resulting in lower projection

Table 2 *Recoil results.*

Test	Article identification	Effect	Number of shots	Recoil characteristics					Duration/s
				Peak force/lbf		Interval/s			
				Min	Max	Min	Max	Avg	
1	A	Report	49	34	72	0.8	2.2	1.31	64
2	B	Star shell	19	29	69	0.9	2.2	1.42	27
3	A	Report	49	25	85	0.6	2.0	1.37	67
4	B	Star shell	19	38	84	0.5	2.4	1.42	27
5	B	Star shell	19	37	90	0.9	2.5	1.37	26
6	B	Star shell	19	28	100	0.9	2.6	1.37	26
7	A	Report	49	10	95	0.8	0.9	1.39	68
8	A	Report	49	16	97	0.9	3.1	1.39	68
9	A	Report	49	36	145	0.8	2.0	1.24	61
10	A	Report	49	13	110	0.8	1.6	1.45	71
11	C	Multiple effects	50	67	>100	0.3	30	1.44	72
12	C	Multiple effects	50	67	211	0.1	2.1	0.92	46
13	D	Multiple effects	49	23	277	0.4	13.8	1.00	49
14	E	Multiple effects	49	48	212	0.3	1.8	0.94	46
15	F	Multiple effects	49	255	>420	0.8	1.2	0.16	8

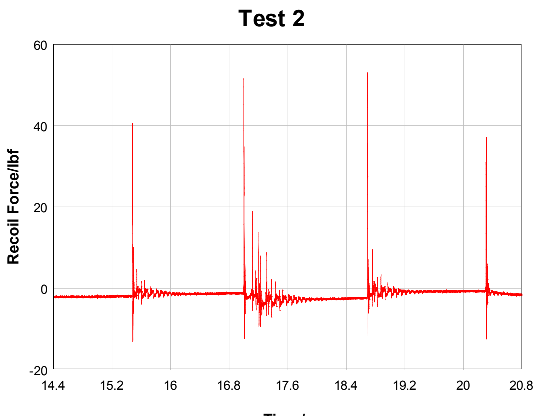

Figure 5. *Sequential shots (Shots #11–14).*

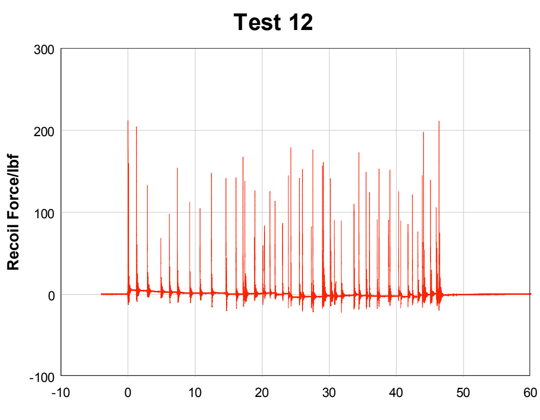

Figure 6. *Complete history of a 50-shot cake (Article C).*

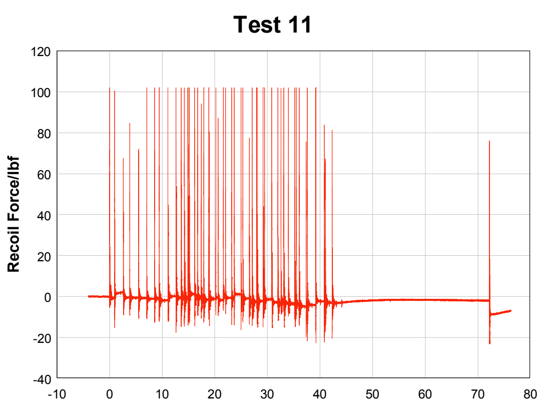

Figure 7. *Long inter-shot delay (end).*

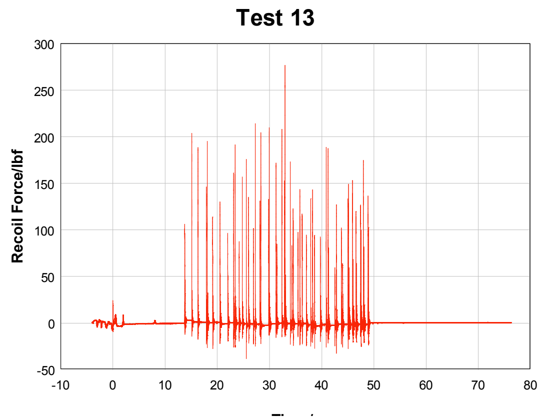

Figure 8. *Long inter-shot delay (beginning).*

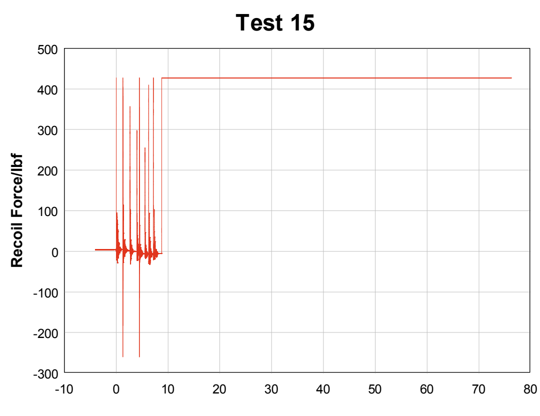

Figure 9. *Malfunction (mass explosion of remaining effects of Sample F).*

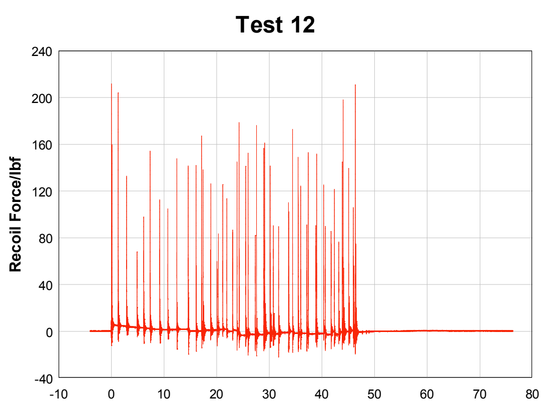

Figure 10. *Rapid firing record.*

heights and recoil forces.

Defects and malfunctions were observed in 3 of the 15 tests. Two articles had extremely long delays between shots and the third ceased functioning after eight shots fired. These malfunctions are shown in Figures 7 to 9.

Figure 7 shows a long delay between the initial group of shots and the last one while Figure 8 shows a long delay before the first and subsequent shots.

The RLP also provided a record (Figure 9) of the malfunction in Test 15 where the 49-shot article stopped functioning just after the eighth shot.

Articles of this type, depending on the design of the delay fusing, may also fire effects in very rapid succession making it difficult for the observer to determine timing. The recoil records provided a method for evaluating this timing. In at least one case several effects fired rapidly. This can be seen upon closer examination of the recoil history of Test 12 shown in Figure 10 and expanded in Figure 11. It is difficult to determine the number of individual shots from the original record. The expanded view clearly shows individual firings at as little as 100 ms apart.

Conclusions and Recommendation

The use of a load cell assembled as a Recoil Load Platform (RLP) proved to have value in the evaluation of multi-shot type devices. Evaluation of such devices is sometimes difficult due to their complexity compared to simple fireworks with single effects. The recoil records allow determination of inter-tube firing intervals and durations, and provide proof of malfunctions such as long delay times or duds.

The data obtained from the RLP are useful and should be considered for routine testing, even though it requires additional time for data analysis. It would also be useful to repeat tests using video to track the projection heights so as to correlate them to the recoil force of each shot.

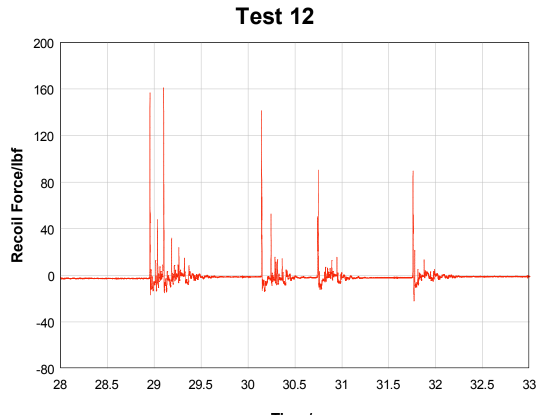

Figure 11. *Expansion of trace record.*

References

1 *Consumer and Display Fireworks Criteria, Authorization, Sampling, Composition, General and Detailed Requirements for 7.2.1 and 7.2.2, Revision 4*, Natural Resources Canada, September 1, 2004.

2 E. Contestabile, R. Guilbeault and D. Wilson, *Loads Resulting from the Recoil of Fireworks Mortars*, 4th International Symposium on Fireworks, Halifax, 1998.

3 K. King, E. Contestabile, K. Hanasaki, R. Guilbeault, A. Rae and J. Collinsworth, *Response of Typical Roof Structures to Recoil Loads from Fireworks Shell Launch*, 9th International Symposium on Fireworks, Berlin, Germany, 2005.

Survey of Firework Trends from UK Display Companies

Tom Smith and Avril diPalma
Davas Ltd, 8 Aragon Place, Kimbolton, Huntingdon, Cambs, UK PE28 0JD

Abstract: *As part of Davas's involvement with the UK firework display industry, a survey of UK professional firework display companies was carried out to identify areas of current concern and to attempt to identify trends. The results of this survey are presented here.*

Keywords: *Survey, 2007, fireworks, UK*

Introduction

Although it has been suggested many times before, the firework industry is probably under greater threat now than it has been for many years.

As part of the authors' involvement with the UK's Explosive Industry Group (EIG)[1] and the British Pyrotechnists Association (BPA)[2] a survey of the UK display firework companies was carried out to identify areas of current concern, and in attempt to identify future trends. It is intended that the survey be carried out on a regular basis, adopted as necessary to reflect changes in regulation and practice, in order to try and map these trends.

The UK Industry

The UK professional firework display industry is quite diverse, ranging from operations that perform only a handful of displays each year to those that operate all year round staging many hundreds of displays. Recent work by Davas Ltd with the UK Government[3] has quantified the professional display industry as shown in Table 1.

The UK display industry, like many around the world, perceives the threat to their businesses as deriving from many sources, be they legislative or related to practice or supply.

Table 1. *UK Firework display industry statistics.*

No. of display companies	180
No. of manufacturers	1
No. of importers	26
Total number of displays	*ca*. 10000
Total value of displays (£)	*ca*. 20 million
No of companies surveyed	98

Determination of questions

The questions posed to the companies are presented in Tables 2A–H. The topics to be examined and the indicative responses were determined to reflect issues arising from meetings of the EIG and BPA.

Scope of survey

98 UK display companies were surveyed by email and respondents asked to provide a rating of each indicative response by rating each answer 1–10 (10 being the greatest). Nil responses were acceptable, and respondents were also asked to provide further information or further indicative responses, and also to suggest topics for future surveys.

It is proposed that in future it may be useful to extend the survey worldwide and also to other sectors of the firework industry – for instance those that specialise in supply of fireworks to the public. In addition, it would be interesting to compare the responses from industry and from enforcing authorities.

Survey period

The survey was carried out in the period 1 June 2007 to 20 June 2007

Results and Discussion

The results are presented in the following tables (Table 2A–H). Each table quantifies the answers received in 2 ways – respectively

- The maximum value given by any respondent to the question and answer
- The average value given by all respondents to the question and answer

		Maximum	Average
A – International legislation	(a) The EU Pyrotechnic Directive ( )	10	6.9
– Which of the following will have the greatest effect in the short/medium term?	(b) Changes to the UN classification regime ( )	10	9.0
	(c) Regulations on the use of pyrotechnics ( )	8	5.9
	(d) Environmental legislation ( )	8	5.4
	(e) Transport Security ( )	7	5.0
	(f) Other – please specify below		

		Maximum	Average
B – Products (fireworks)	(a) Single shot – comets ( )	10	7.8
– Please indicate which product types you think will find increased application in the short/medium term?	(b) Single shot – other items ( )	10	7.4
	(c) Mines ( )	8	6.5
	d) Multishot devices ("cakes") – traditional ( )	8	6.0
	(e) Multishot devices ("cakes") – novel designs ( )	8	7.6
	(f) Spherical burst shells ( )	7	4.6
	(g) Non-spherical burst shells ( )	8	4.6
	(h) Static or dynamic "set pieces" ( )	8	5.5
	(i) Lancework devices ( )	10	5.4
	(j) Low noise effects ( )	10	8.3
	(k) Daylight effects ( )	8	4.5
	(l) Pyrotechnic effects used as fireworks ( )	10	5.4
	(m) Other – please specify below		

		Maximum	Average
C – New developments	(a) Nano compositions ( )	6	4.4
– Which of the following developments will have the greatest impact on fireworks in the short/medium term?	(b) Use of novel oxidisers ( )	8	6.2
	(c) Blackpowder alternatives ( )	10	6.1
	(d) Flashpowder alternatives ( )	10	8.1
	(e) Biodegradable components ( )	9	7.0
	(f) Use of novel colorants ( )	9	6.1
	(g) Other – please specify below		

The major issues, with average scores over 7.5, therefore are:

- Changes to the UN classification of fireworks
- Increased use of single shot comets
- Increased use of novel design "cakes"
- Increased use of low noise effects
- Alternatives to flashpowder
- Environmental aspects of the use of plastic sub-components
- Environmental aspects of the use of metal sub-components
- Issues concerning the supply of igniter cord or equivalent
- Issues arising from the use of low quality igniters

None of these is surprising, but we hope they will serve as a useful benchmark for future studies. In addition it is useful to attempt to quantify concerns rather than rely on anecdotal evidence.

Other topics

Other topics of concern, and areas for future

		Maximum	Average
D – Environmental concerns	(a) General debris (mess) arising from the use of fireworks or pyrotechnics ( )	8	5.3
– Please rate the following as to which poses the greatest environmental concern in the short/medium term?	(b) Use of plastic sub-components ( )	10	7.6
	(c) Use of metal sub-components ( )	10	8.1
	(d) Noise arising from use of fireworks or pyrotechnics ( )	10	6.8
	(e) Toxic combustion by-products from firing displays – environmental issues ( )	9	6.0
	(f) Use of heavy metal salts ( )	8	5.9
	(g) Use of perchlorates ( )	8	5.3
	(h) Toxic combustion by-products from firing displays – health issues ( )	8	4.5
	(i) General effect on flora/fauna ( )	7	3.8
	(j) Other – please specify below		

		Maximum	Average
E – Restriction of products	(a) Electric igniters ( )	10	4.5
– Please rate the difficulty in obtaining the following items and which could, therefore, restrict your operation in the short/ medium term?	(b) General fuse – such as pipe match ( )	10	3.6
	(c) Igniter cord or equivalent ( )	10	7.9
	(d) Pyrotechnic delays ( )	10	4.3
	(e) Any item containing flashpowder ( )	10	6.1
	(f) Blackpowder ( )	10	3.7
	(g) Other – please specify below		

		Maximum	Average
F – Safety	(a) Increased use of electric firing systems ( )	10	3.4
– How great are your concerns about display safety or operation in the short/medium term?	(b) Use of low quality igniters ( )	10	7.6
	(c) Mortar construction methods ( )	9	5.8
	(d) Mortar racking systems ( )	9	6.9
	(e) Prescribed crowd safety distances ( )	10	6.6
	(f) Terrorist/protestor activities ( )	6	3.4
	(g) Effects of climate change – eg weather ( )	10	3.6
	(h) Changes to daylight saving time ( )	7	3.7
	(i) Other – please specify below		

surveys to address, identified by the respondents include the following:

- Use of close proximity effects
- Compliance costs issues
- Equitableness of enforcement – those companies that have the highest profiles are policed more heavily than those that maintain a "low profile"
- Storage of UN 0333 (1.1G) fireworks
- Security of fireworks in transport
- Qualifications for drivers
- "Stabling" of explosives vehicles on long journeys
- Entry criteria for new companies in the professional display market
- Restrictions on who may import

		Maximum	Average
G – Domestic issues	(a) Training of firers ( )	10	5.3
– Please rate the impact of the following on your business in the short/medium term?	(b) Changes to storage regulations ( )	9	5.5
	(c) Changes to transport regulations ( )	9	5.9
	(d) Changes in supply regulations ( )	8	5.9
	(e) Changes to use regulations ( )	8	5.1
	(f) Difficulties in supply – domestic ( )	9	3.8
	(g) Difficulties in supply – international ( )	9	4.0
	(h) Other – please specify below		

H – Other **– Please indicate any other aspects you consider will affect the industry in the short/medium term, or which you feel should be included in future surveys.**	

Conclusions

The UK firework display industry has highlighted the areas of current concern to them, which probably reflect the concerns worldwide.

Future iterations of the survey will attempt to address the highlighted concerns and extend its scope to enable comparisons

- Between countries
- Between users and enforcers.

Acknowledgements

The assistance of members of the EIG and BPA is gratefully acknowledged.

References

1 See http://www.eig.org.uk

2 See http://www.pyro.org.uk

3 This research forms part of an ongoing project between the following UK authorities – Health & Safety Executive (www.hse.gov.uk) and the Local Authority Coordinating Body on Regulatory Services (LACoRS – http://www.lacors.gov.uk)

Thermal Conductivity Testing of Minimal Volumes of Energetic Powders†

Adam Harris[a] and Daniel N. Sorensen[b]
[a] Mathis Instruments Ltd., 21 Alison Blvd., Fredericton, NB E3C 2N5, Canada
Email: aharris@cvision.ca
[b] Naval Surface Warfare Center Indian Head Division, 101 Strauss Ave, Indian Head, MD, USA 20640-5035

Abstract: *Safety constraints have traditionally presented researchers with challenges in testing the thermal conductivity of energetic powdered materials. Minimal volumes of energetic powders can now be tested with the modified transient plane source technique. The newly modified sensor design further reduces the possibility of impact, friction and electrostatic discharge (ESD) hazards. This paper will present results generated in testing ammonium perchlorate (AP).*

Keywords: *thermal conductivity, transient plane source, energetic powder, electrostatic discharge*

Introduction

Testing the thermal conductivity of most energetic powder materials is a challenge with traditional steady-state techniques, as the required large volumes of material pose undesirable safety risks or the necessary sample geometries are impractical. This often leads to estimation of thermal conductivity in predictive models rather than actual measurement. The dependence of thermal conductivity of a material undergoing an exothermic reaction on local temperature has a significant effect on the critical conditions for thermal ignition.[1] The theory of thermal ignition, whether or not consumption and diffusion of reactant is taken into account, has been commonly analyzed using the traditional grouping of dimensionless parameters suggested by Frank-Kamenetskii (1955).[2] The theory assumes that the heat generation inside a body follows an Arrhenius model:

$$q' = Q\rho A e^{-\frac{E}{RT}} \qquad (1)$$

where
Q is the heat of reaction [kJ g^{-1}]
ρ is the bulk density of the material [kg m^{-3}]
A is the pre-exponential factor [s^{-1}]
R is the universal gas constant [8.314 J mol^{-1} K^{-1}]
E is the apparent activation energy [J mol^{-1}]
T is the temperature [K]
q' is the heat generation rate per unit volume [J s^{-1} m^{-3}]

From this, Frank-Kamenetskii developed the following expression, where the non-dimensional heat generation is found:[3]

$$\frac{\rho Q A}{\lambda}\frac{EL^2}{RT_0}e^{\frac{-E}{RT_0}} = \delta \qquad (2)$$

where
λ is the thermal conductivity of the material
L is the characteristic length of the given body (the half side length for cubes).
T_0 is the ambient temperature [K]

In the present study, the modified transient plane source technique was applied to measure the thermal conductivity of an energetic material directly as an alternative to the book values that are frequently substituted in the computational models based on the aforementioned theory.

† Approved for public release, distribution is unlimited.

Paper as originally presented at NATAS 2006.

Figure 1. *Mathis TCi Thermal Conductivity Analyzer.*

Experimental

Apparatus

The Mathis TCi™ system utilized in the study to perform the thermal conductivity measurements is shown in Figure 1.

This thermal conductivity measurement device is based on the modified transient plane source technique. It uses a one-sided, interfacial, heat reflectance sensor that applies a momentary, constant heat source to the sample. The difference between this method and traditional hot wire techniques is that the heating element is supported on a backing, which provides mechanical support, electrical insulation and thermal insulation. This modification eliminates the intrusive nature of the hot wire method and provides the capability to test smaller volumes of material as the wire is coiled as pictured in Figure 2.

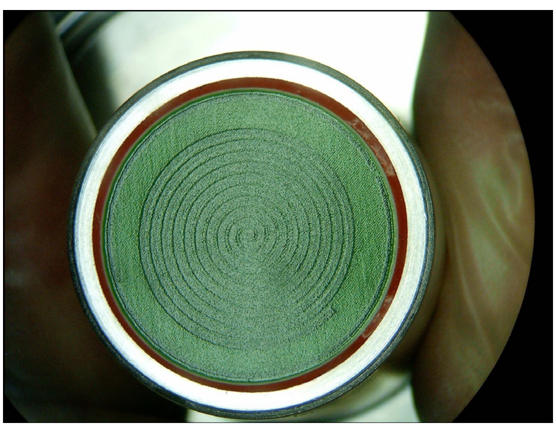

Figure 2. *Sensor face – diameter is 17 mm.*

The associated test method enables the testing of solids, liquids, powders and pastes without melting or otherwise modifying the sample to conform to the geometry of the test cell. The sample is tested by placing it in intimate contact with the heating element of the sensor for a resident amount of time of typically 1 to 3 seconds. A known current is applied to the sensor's heating element providing a small amount of heat. The heat provided results in a rise in temperature at the interface between the sensor and the sample – typically less than 2 ºC. This temperature rise at the interface induces a change in the voltage drop of the sensor element. A typical voltage data chart is displayed in Figure 3.

Since the rate of temperature rise at the heating element is inversely proportional to the thermal conductivity of the material, this material property can be determined by measuring the rate of voltage rise when a constant current is applied.[4] Voltage increase can be correlated with thermal conductivity through a calibration with reference

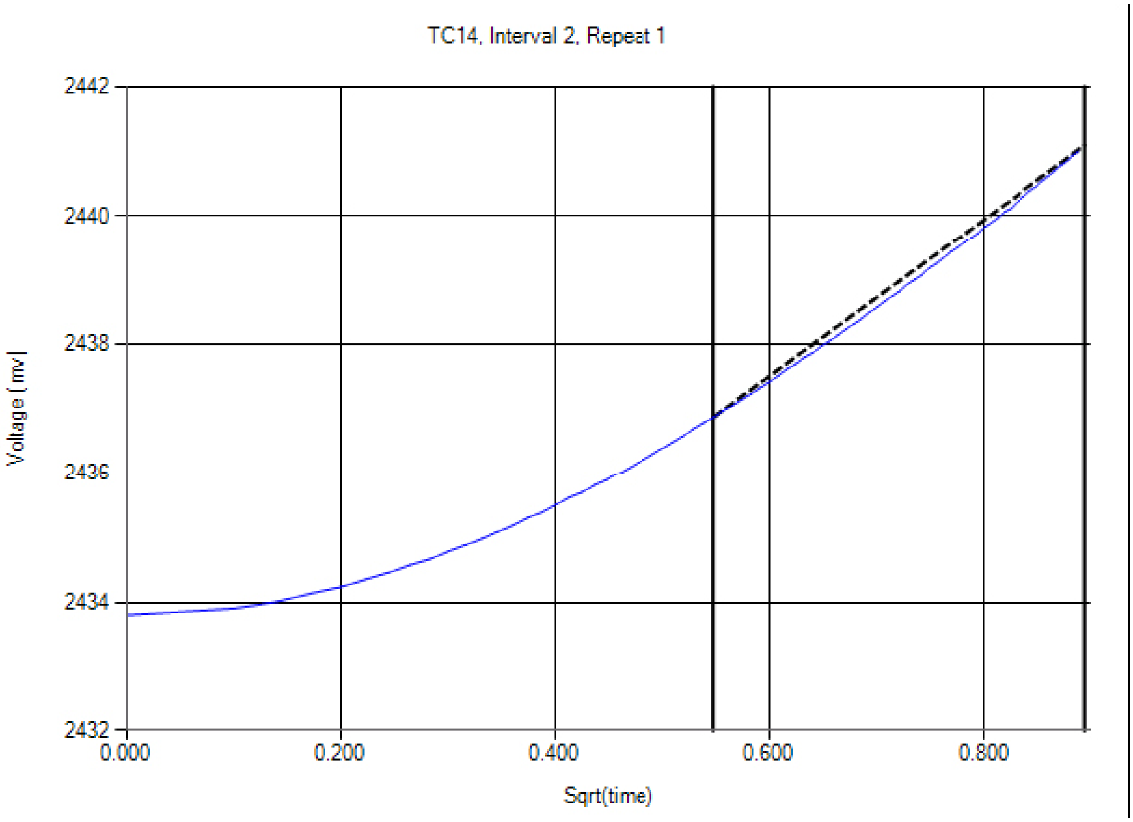

Figure 3. *Voltage data chart.*

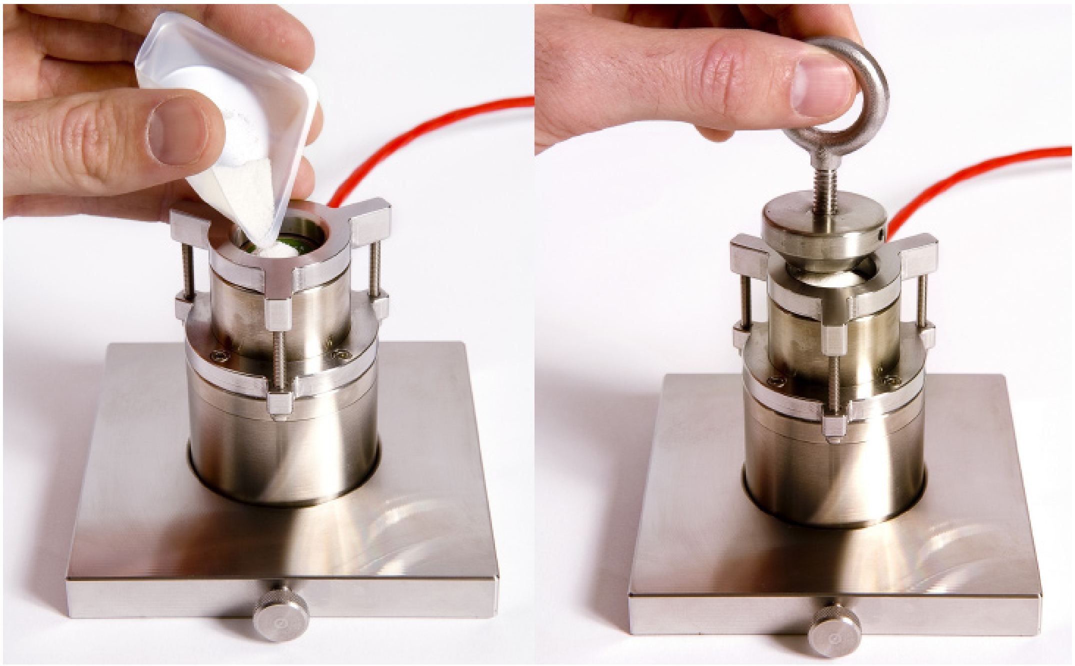

Figure 4. *TCi small-volume test cell.*

Table 1 *Test results – ammonium perchlorate [relative standard deviation (RSD)].*

Test	Thermal conductivity/ W m^{-1} K^{-1}	Average/W m^{-1} K^{-1}, $N = 4$	RSD (%), $N = 4$	Average/W m^{-1} K^{-1}, $N = 3$	RSD (%), $N = 3$
1	0.127086	0.1276	0.31%		
	0.127641				
	0.127866				
	0.127969				
2	0.130499	0.1293	0.64%	0.1288	0.75%
	0.128595				
	0.128970				
	0.129272				
3	0.129295	0.1293	0.38%		
	0.129967				
	0.128839				
	0.129063				

materials having known thermal conductivity. From this calibration, the conductivity of unknown materials can be determined.[5] The more thermally insulative the material is, the steeper the voltage rise. Additional work was needed to configure the sensor to accommodate US Navy energetics needs.

Many energetic powders are sensitive to initiation via impact, friction or electrostatic discharge (ESD).

A specially designed sensor test cell was constructed to minimize the effect of these hazards. The test cell was designed such that it can be rigidly attached to the sensor while diminishing the possibility of powder going into screw holes which are potential impact and friction hazards. Further, the sensor head design also allowed grounding leads to the test cell, cap, and sensor so that ESD effects could be minimized.

The grounding wire could then be attached to the building's grounding system. Figure 4 shows the sensor head without the attached grounding leads.

Materials

Ammonium perchlorate (NH_4ClO_4) was used as received with a nominal particle size of 200 µm. The salt is a common energetic component in US Navy weapons systems.

Methods

The small-volume test cell pictured in Figure 4 is filled with approximately 3/8 teaspoon (1.9 ml) of ammonium perchlorate. Care is taken to avoid compaction of the powder prior to placing the test cell cap.

An accuracy check was performed on the instrument prior to running any tests on a standard reference material and confirmed the instrument was performing well within the stated accuracy specification of 5%.

Results

A summary of the results is provided in Table 1 and graphically in Figure 5. For all measurements, the instrument demonstrated a precision better than 1%.

Accuracy test

An accuracy check was performed on the instrument prior to running any tests on a standard reference material and confirmed the

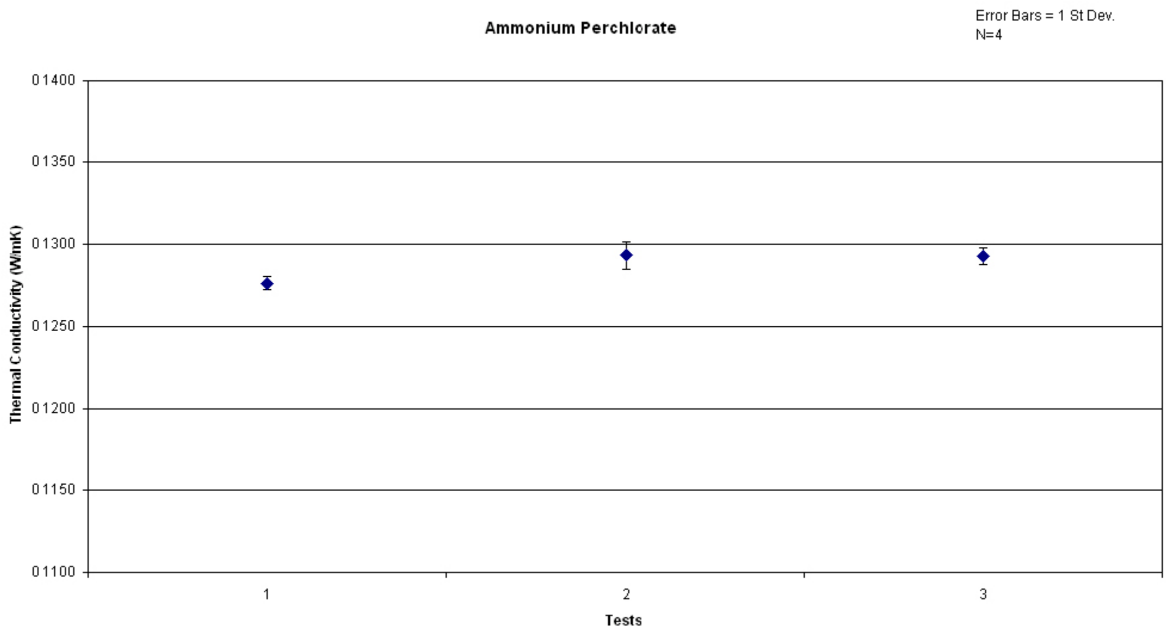

Figure 5. *Results of AP Analyses.*

instrument was performing well within the stated accuracy specification of 5%. The accuracy of the measurements conducted under specific environmental conditions can be examined by measuring calibration materials with externally certified thermal conductivity values under such specific environmental conditions. In comparing the observed measurements of the materials with the known thermal conductivity values of the materials, the accuracy of the measurements for unknown samples can be evaluated. In this study, PDMS (DiMethyl PolySiloxane silicone fluid) was used as the calibration standard to assess the accuracy of the measurements carried out in this study. The results are listed in Table 2.

Conclusions

The thermal conductivity of a volume of approximately 3/8 teaspoon of ammonium perchlorate was measured with an accuracy of better than 2.5%. Further studies are recommended to investigate the relationship between particle size, moisture content, and packing density on the thermal conductivity.

Table 2. *Accuracy test results vs. certified values.*

Sample	Measured k/W m^{-1} K^{-1}	Average of measured k/W m^{-1} K^{-1}	RSD (%)	Real k/W m^{-1} K^{-1}	Accuracy (%)
	0.162194				
	0.162951				
PDMS	0.162945	0.162865	0.24%	0.159	2.43%
	0.163008				
	0.163226				

Acknowledgements

The Other Procurement, US Navy Quality Evaluation Technologies and Equipment program purchased the thermal conductivity instrument and provided funds for this study.

References

1 A. A. Lacey and G. C. Wake, Thermal Ignition with Varial Thermal Conductivity, *IMA Journal of Applied Mathematics*, vol. 28, pp. 23–39.

2 J. G. Burnell, J. G. Graham-Eagle, B. F. Gray and G. C. Wake, Determination of Critical Ambient Temperatures for Thermal Ignition *IMA Journal of Applied Mathematics*, vol. 42, pp. 147–154.

3 M. A. Pauner and H. Bygbjerg, Spontaneous ignition in storage and production lines Part 3: Investigation of protein powder, HP500 Danish Institute of Fire and Security Technology (DIFT) Report, 2005:05.

4 X. Qiu, K. Schmidt and N. E. Mathis, Thermal Conductivity of Thin Films, *Proceedings of the North American Thermal Analysis Society Conference*, October 2004, Virginia, USA, p. 41.

5 X. Qiu, K. Schmidt, A. Harris and G. Chaplin, The Characterization of Thermal Interface Materials using Thermal Conductivity for Within Sample and Batch to Batch Variation Analysis, *Proceedings of the North American Thermal Analysis Society Conference*, 2005, Los Angeles, USA.

Book Reviews

Introduction to Fireworks

T Yoshida and D Ding

Reviewed by

Theodore S. Sumrall

Associate Editor, Science and Technology of Energetic Materials
Adjunct Professor, University of Florida Department of Engineering
Former Liaison Officer, Air Force Office of Scientific Research – Tokyo Detachment

Introduction to Fireworks is an excellent text and reference manual for scientists and engineers involved in energetic material research and development. Professors Yoshida and Ding cover all of the important aspects of the subject and even delve into the historical aspects of the art as far back as the dawn of the Christian era when gunpowder was discovered in China, carried into Europe and experimented upon by Roger Bacon in the 13th Century. The fireworks community has long needed a text to allow novices to be able to quickly understand the principles behind this important (and sometimes dangerous) field of energetic materials. Careful study of this text will allow researchers to avoid many of the costly mistakes associated with energetic material formulation, development and testing while achieving the desired objectives in a timely manner.

Bombs and Bombings, A Handbook to Protection, Security, Detection, Disposal, and Investigation for Industry, Police, and Fire Departments, Third Edition.

Brodie, Thomas G.

Charles C. Thomas Publisher, Ltd, Springfield IL
2005, 316pp.

Reviewed by Megan Bottegal, BS. and Bruce McCord, PhD. Department of Chemistry and Biochemistry, Florida International University, Miami, FL 33199, USA

This book is an overview of the vast and personal experience Captain Thomas Brodie has accumulated in twenty-four years as a founder of the Miami Bomb squad and supervisor of its crime scene unit. Over the course of his career, Captain Brodie investigated approximately 350 bombings and assisted in the disposal of over 4000 bombs and tons of explosives. He is a charter member of the International Association of Bomb Technicians and Investigators and among other awards and honors, he was knighted by the Queen Elizabeth II for his role in protecting the British Empire in the Caribbean. Captain Brodie's experiences arise from his role in developing, adapting, and utilizing a variety of tools for bomb detection, disruption and disposal during his service to the city of Miami, and the counterterrorism community.

The book is organized in a variety of chapters covering issues from how to organize and equip a bomb squad to sections on types of explosive devices and legal issues. The text also covers techniques for finding, disrupting and disposing of bombs, explosive materials, and detonators. It concludes with sections on evidence collection, including checklists for workers in the field and an overview of the principles of bomb protection.

Over his years of service to the Miami Bomb squad Captain Brodie was kept busy investigating bombs and bombings resulting from violent Cuban exile groups, custom interdictions, criminal bombings and property crimes. He speaks with distinctive and personal experience on the methods for dealing with these situations. Thus, the sections in the book on methods for disarming and disruption of explosive devices are especially well done. Captain Brodie has personally developed a number of techniques for bomb disposal and clearly describes the advantages and disadvantages of different modes of their operation. He also provides detailed descriptions of the operational procedures he and others have developed, and includes personal anecdotes that help emphasize each point.

The book contains extensive illustrations using black and white photographs of actual devices that the author has investigated and rendered safe. These photographs should prove extremely valuable in training new investigators on the types of evidence that may be collected from the scene. Other photographs include crime scenes, injuries to victims, and post-blast damage and are equally instructive. Also valuable are the sections in the book on how to properly organize and interface a bomb squad into the overall operation of a public safety program. These sections demonstrate prescient insight into the current problems of organizing states and communities for disaster preparedness and homeland security.

The book as written is more a series of overall guidelines for bomb disposal units than a handbook as it lacks the large appendix of references and resources commonly present in most handbooks of this sort. Hopefully the next edition will include such materials which will help the reader further examine the various useful tips and resources mentioned in the text. Also, the book would benefit from improved editing, as certain topics mentioned in the book could be more clearly defined and organized.

However, these are minor complaints when taken against the overall usefulness and descriptive value of the book. In general, there is a wealth of important information on all aspects of bomb investigation and disposal. Captain Brodie astutely recognizes that implementing standardized guidelines in the areas of equipment, training, organization, and procedures is vital, not just for bomb squad personnel, but also for management and administration to ensure the safest methods of bomb protection. This book is therefore a must read for anyone involved in bomb disposal, and should also be valuable resource for all persons involved the collection, analysis and prosecution of bombing incidents.

Events Calendar

Pyrotechnics and Fireworks

34th International Pyrotechnics Seminar
October 8 - 11 2007, Beaune, France
web: http://www.afpyro.org

35th International Pyrotechnics Seminar
July 13 - 18 2008, Fort Collins. CO, USA
Contact: Linda Reese, Appl. Res. Assoc. Inc.
10720 Bradford Road., Ste 110
Littleton, CO 80127, USA
Phone: +1-303-795-8106
Fax: +1-303-795-8159
email: lreese@ara.com
web: http://www.ipsusa.org

Pyrotechnics Guild Int'l Convention
4-10 August, 2007
Contact: Frank Kuberry, Sec. Treas.
304 W Main St
Titusville, PA 16354, USA
Phone: +1-814-827-6804
email: kuberry@earthlink.net
web: http://www.pgi.org

Listing of Fireworks Events - Worldwide
web: http://fireworksguide.com

Pyrotechnic Chemistry Lecture Course
14/15/16 April 2008
Huntingdon, Cambs. UK
For more information please see
web: http://www.pyrochemistry.net

Energetic Materials

38th International Annual Conference Energetic Materials
June 26 - June 29, 2007, Kahlsruhe, Germany
Phone: +49 721 46 40-201
email: yvonne.hofmannict@fraunhofer.de
web: http://www.ict.fraunhofer.de/english/events/anconf/index.html

11th International Seminar "New Trends in Research of Energetic Materials"
Apríl 09-11, 2008
Contact: Prof. Svatopluk Zeman and Mr. Jan Ottis, Institute of Energetic Materials, University of Pardubice, CZ-532 10 Pardubice, Czech Republic, European Union,
Phone: +420 46 603 8023
Fax: +420 46 603 8024,
email: seminar@ntrem.com,
svatopluk.zeman@upce.cz
ottis@ntrem.com
web: www.ntrem.com

High Power Rocketry

LDRS 2007
Contact: see web site
web: http://www.tripoli.org/calendar.htm

Model Rocketry

NARAM 2007
Contact:
web: http://www.naram.org
For other launch information visit the NAR Web site: http://www.nar.org

Future Events Information

If you have information concerning future explosive, pyrotechnics or rocketry meetings, training courses or other events that you would like to have published in the Journal of Pyrotechnics and on the website http://archives.jpyro.com - please provide the following information: Name of event, Date and place (City, State, Country), Contact information - including, if possible, name of contact person, postal address, telephone and fax numbers, email address and website

Sponsors

Individual Sponsor

Gerald Laib
17611 Longview Lane
Olney, MD 20832, USA
phone: 301-744-4358
fax: 301-744-4784

Corporate Sponsors

Allied Speciality Insurance
Rick D'Aprile
10451 Gulf Blvd.
Treasure Island, FL 33706, USA
phone: 800-237-3355
fax: 727-367-1407
email: info@alliedspeciality.com
web: http://www.alliedspeciality.com

American Fireworks News
Jack Drewes
233 Silver Lake Rd, Dingmans Ferry, PA 18328, USA
phone: 570-828-8417
fax: 570-828-8695
email: afn@fireworksnews.com
web: http://www.fireworksnews.com

American Pyrotechnics Association
Julie Heckman
4808 Moorland Lane - Ste 109, Bethusda, MD 20814, USA
phone: 301-907-8181
fax: 301-907-9148
email: jheckman@americanpyro.com
web: http://www.americanpyro.com

Brooke * Mawhorr, PC
Douglass K Mawhorr
112 East Gilbert St., PO Box 1071
Muncie, IN 47305, USA
phone: 765-741-1375
fax: 765-288-7763
email: dmawhorr@aol.com

Canadian Explosives Research Laboratory
Dr Phil Lightfoot, Manager
CANMET - 555 Booth St., Ottawa, ON K1A 0G1, Canada
phone: 613-947-7534
fax: 613-995-1230
email: plightfo@nrcan-nrcan.gc.ca
web: http://www.nrcan.gc.ca/mms/cerl

Combined Specialities International Inc.
John & Alice Allen
8362 Tamarack Village, Ste. 119,
Woodbury, MN 55125, USA
phone: 651-855-0091
fax: 651-855-0088
email: jallen@combinedspecialities.com

Davas Ltd
Tom Smith
8 Aragon Place, Kimbolton, Huntingdon,
Cambs. UK. PE28 0JD
phone: +44 1480 860124
fax: +44 1480 861125
email: toms@davas.co.uk
web: http://www.davas.co.uk

Daveyfire, Inc.
Alan Broca
2121 N California Blvd. Ste. 290,
Walnut Creek, CA 94596, USA
phone: 925-926-6414
fax: 925-926-6439
email: info@daveyfire.com

Delcor Industries Inc
Sam Bases
19 Standish Ave., Yonkers, NY 10710, USA
phone: 914-779-6425
fax: 914-779-6463
email: delcor@hotmail.com
web: http://www.delcorind.com

Firelinx, Inc.
David Russell
PO Box 8274, Incline Village, NV 89452, USA
phone: 775-832-5522
fax: 775-684-7652
email: larrymat@firelinx.us
web: www.firelinx.us

Fire One
Dan Barker
863 Benner Pike, State College, PA 16801, USA
phone: 814-238-5334
fax: 814-231-0799
email: info@fireone.com
web: http://www.fireone.com

Firefox Enterprises Inc.
Gary Purrington
11612 N Nelson, Pocatello, ID 83202, USA
phone: 208-237-1976
fax: 208-237-1976
email: custserv@firefox-fx.com
web: http://www.firefox-fx.com

Firework Professionals
Anthony Leyland
PO Box 19-912, Christchurch, 8030, New Zealand
phone: +64-3-982-3473
fax: +64-3-982-3474
email: firework@firework.co.nz
web: http://firework.co.nz

Fireworks
PO Box 40, Bexhill, Sussex TN40 1GX, England
phone: +44-1424-733-050
fax: +44-1424-733-050
email: editor@fireworks-mag.org
web: http://www.fireworks-mag.org

Fireworks and Stage FX America
Joseph R. Bartolotta
PO Box 488, Lakeside, CA 92040, USA
phone: 619-938-8277
fax: 619-938-8273
email: info@fireworksamerica.com
web: http://www.fireworksamerica.com

Fireworks Business
Jack Drewes
233 Silver Lake Rd, Dingmans Ferry, PA 18328, USA
phone: 717-828-8417
fax: 717-828-8695
email: afn@fireworksnews.com
web: http://www.fireworksnews.com

Fireworks by Grucci
Phil Grucci
1 Grucci Lane, Brookhaven, NY 11719, USA
phone: 631-286-0088
fax: 631-286-9036
email: philgrucci@aol.com
web: http://www.grucci.com

Fullam's Fireworks Inc
Rick Fullam
PO Box 1808 CVSR, Moab, UT 84532, USA
phone: 435-259-2666
email: rfullam_3@yahoo.com

Geelong Fireworks
Steve Lawrence
PO Box 1394, Geelong 3220, Australia
Phone: +61-3-5244-3764
email: admin@geelongfireworks.com.au

Goex Inc.
Mick Fahringer
PO Box 659, Doyline, LA 71023, USA
phone: 318-382-9300
fax: 318-382-9303
email: email@goexpowder.com
web: http://www.goexpowder.com

Island Fireworks Co. Inc.
Charles Gardas
N735 825th St, Hager City, WI 54014, USA
phone: 715-792-2283
fax: 715-792-2640
email: islndfwk@pressenter.com
web: http://www.island-fireworks.com

Lantis Fireworks & Lasers
Ken Lantis
PO Box 491, Draper, UT 84020, USA
phone: 801-768-2255
fax: 801-768-2433
email: info@fireworks-lasers.com
web: http://www.fiireworks-lasers.com

MagicFire Inc
Paul McKinley
PO Box 896, Natick, MA 01760, USA
phone: 508-647-9645
fax: 508-647-9646
email: pyrotech@magicfire.com
web: http://www.magicfire.com

Martin-Baker Aircraft Ltd
David Chapman
Lower Rd, Higher Denham, Uxbridge, Middlesex UB9 5AJ
Great Britain
Phone: 44-1895-836-644
FAX: 44-1985-836-686
email: dchapman@martin-baker.co.uk
web: www.martin-baker.com

Martinez Specialities
Phil Martinez
208 Bossard Rd, Groton, NY 13073, USA
phone: 607-898-3053
fax: 607-898-3952
email: mr.squib@clarityconnect.com

Maratamaya Ogatsu Fireworks Co. Ltd.
1-35-35 Oshitate Fuchu, Tokyo, 183-0012, Japan
phone: +81 42-363-6251
fax: +81-42-363-6252
email: hanabi@mof.co.jp
web: http://www.mof.co.jp

Mighty Mite Marketing
Charlie Weeth
122 S 17th St, LaCrosse, WI 54601, USA
phone: 608-784-3212
fax: 608-782-2822
email: czweeth@pyro-pages.com
web: http://www.pyro-pages.com

MP Associates Inc.
PO Box 546, Ione, CA 94640, USA
phone: 209-274-4715
fax: 209-274-4843

Nilsson & Lee Pyrotechnics
Hans Nilsson
Box 130, SE-372 22 Ronneby, Sweden
phone: +46-457-15600
email: info@pyrokits.com
web: http://www.pyrokits.com

Nitrotech Australia Pty. Ltd.
Chris Larkin
PO Box 349, Mount Isa, QLD 4825, Australia
phone: 617-47-44-2290
fax: 617-47-44-3998
email: nitrotech@smartchat.net.au

Precocious Pyrotechnics Inc.
Garry Hanson
4420 278th Ave NW, Belgrade, MN 56312, USA
phone: 320-346-2201
fax: 320-346-2403
email: ppinc@tds.net
web: http://www.pyro-pro.com

Pyro Shows Inc.
Lansden Hill
PO Box 1406, LaFollette, TN 37766, USA
phone: 800-662-1331
fax: 423-562-9171
email: info@pyroshows.com
web: http://pyroshows.com

Pyrodigital Consultants
Ken Nixon
1074 Wranglers Trail, Pebble Beach, CA 93953, USA
phone: 831-375-9489
fax: 831-375-5255
email: pyrodig@aol.com
web: http://www.infinityvisions.com/pyrodigital

PyroLabs Inc.
Ken Kosanke
1775 Blair Road, Whitewater, CO 81527, USA
phone: 970-245-0692
fax: 970-245-0692
email: ken@jpyro.com

RCS Rocket Motor Components Inc.
Gary Rosenfield
2113 W 850 N St, Cedar City, UT 84720, USA
phone: 435-865-7100
fax: 435-865-7120
email: garyr@powernet.net
web: http://www.rocketmotorparts.com

RES Speciality Pyrotechnics
Steve Coman
21595 286th St, Belle Plaine, MN 56011, USA
phone: 952-873-3113
fax: 952-873-2859
email: respyro@earthlink.net
web: http://www.respyro.com

Rozzi Famous Fireworks
Arthur Rozzi
PO Box 5, Loveland, OH 45140, USA
phone: 513-683-0620
fax: 513-683-2043
email: art@rozzifireworks.com
web: http://www.rozzifireworks.com

Service Chemical Inc.
Ben Cutler
2651 Penn Avenue, Hatfield, PA 19440, USA
phone: 215-362-0411
fax: 215-362-2578
email: ben@servicechemical.com
web: http://www.servicechemical.com

Spirit of 76 Fireworks
John Bechtold
6401 West Highway 40, Columbia, MO 65202, USA
phone: 573-477-1776
fax: 573-477-1786
email: marketing@76wholesale.com
web: http://www.76wholesale.com

Starburst Pyrotechnics & Fireworks Displays Ltd
Bonnie Pon
2nd Fl-Sui Hing Hong Bldg-17, Commissioner St
Johannesburg, Gauteng 2000, South Africa
phone: +27-11-838-7705
fax: +27-11-836-6836
email: info@starburstpyro.co.za
web: http://www.starburstpyro.co.za

Strictly FX
Ted Maccabee
1230 Jarvis Ave., Elks Grove Village, IL 60007, USA
phone: 847-290-0272
fax: 847-290-0273
email: website@strictlyfx.com
web: www.strictlyfx.com

Sponsorships

No advertising as such is printed in the *Journal of Pyrotechnics*. However a limited number of sponsors have been sought so that the selling price of the Journal can be reduced from the listed cover price.

Additionally, if you so desire, we will provide a link from the *Journal of Pyrotechnics* website (www.jpyro.com) to the sponsor's website or email address - or simply a company name and contact details.

It is also possible to insert a "flyer" for distribution with the Journal on payment of a modest fee. Please contact the publisher or managing editor for more details.

Information for Readers

Editorial Policy

Articles accepted for publication in the *Journal of Pyrotechnics* can be on any technical subject in pyrotechnics. However, a strong preference will be given to articles reporting on research (conducted by professional or serious individual experimenters) and to review articles (either at an advanced or tutorial level). Both long and short articles will be gladly accepted. Also, responsible letters commenting on past Journal articles will be published along with responses by the authors.

Publication Frequency

The *Journal of Pyrotechnics* appears approximately twice annually, typically in mid-summer and mid-winter.

Subscriptions

Anyone purchasing a copy of the Journal will be given the opportunity to receive future issues on an approval basis. Any issue not desired may be returned in good condition and nothing will be owed. So long as issues are paid for, future issues will automatically be sent. In the event that no future issues are desired this arrangement can be terminated at any time by informing the publisher. Additional discounts are available for payment in advance for issues of the *Journal of Pyrotechnics*. Please contact the publisher for more information.

Back issues

Back issues of the Journal will be kept in print permanently as reference material. These are also available online by subscription at http://archives.jpyro.com

Caution

The experimentation with, and the use of, pyrotechnic materials can be dangerous and may require licences or permits in certain countries; it is felt to be important for the reader to be duly cautioned. Without the proper training and experience no one should ever experiment with or use pyrotechnic materials. Also, the amount of information presented in this Journal is not a substitute for necessary training and experience, nor does it remove the relevant application of national or local laws and regulations.

A major effort has been undertaken to review all articles for correctness. However it is possible that errors remain. It is the responsibility of the reader to verify any information herein before applying that information in situations where death, injury or property damage could result.